tumor suppressor genes during tumorigenesis. Recombination events are not detected by cytogenetic assays. Liechty *et al.* (1998) speculated that the MLA is able to detect recombination because of the autosomal location and the heterozygous status of the *Tk* gene. There is also evidence that the MLA can detect aneuploidy. It is especially important for regulatory purposes to collect more evidence demonstrating that the MLA is capable of detecting aneuploidy and recombination.

For our analysis, we needed mutants that were the result of deletion, mitotic recombination, or aneuploidy. For this purpose, we used three chemicals (AZT, mitomycin C, and taxol) to induce *Tk* mutants. AZT is a thymidine analogue that is clastogenic (Wang *et al.*, 2007). Mitomycin C is a potent clastogen, and it induces mutations in the *Tk* gene (Davies *et al.*, 1993; Dobrovolsky *et al.*, 2002). Taxol can impair cell spindles and induce aneuploidy (Ikui *et al.*, 2005; Mailhes *et al.*, 1999; Schiff and Horwitz, 1980).

As mentioned earlier, Honma *et al.* (2001) performed an analysis of *Tk* mutants using two aneugens, colchicine and vinblastine. The increase in MF was not very high, even after a 24-h treatment (3.6- and 2.3-fold over the control, for colchicine and vinblastine, respectively), so the mutants isolated and analyzed from these chemically treated cultures would include a large number of spontaneous mutants. In the present study, the MFs were much higher (4.8- to 16.6-fold over the control), indicating that many to most of the analyzed mutants were induced by the test chemicals.

Early cytogenetic studies of MLA *Tk* mutants showed that many SC mutants have recognizable chromosome aberrations involving the chromosome 11 that carries the Tk^+ allele. At that time, the chromosome aberrations identified in *Tk* mutants were primarily translocations (Blazak *et al.*, 1986; Hozier *et al.*, 1981; Moore *et al.*, 1985). Later, Southern blot analysis and an allele-specific PCR technique were used to determine the status of the *Tk* allele (Applegate *et al.*, 1990; Liechty *et al.*, 1994, 1996). Most of the SC mutants (both spontaneous and from treated cultures) and a large fraction of LC mutants (depending upon the mutagen) showed the loss of the Tk^+ allele, which indicates that the MLA is able to detect LOH, the most common mutational mechanism in human cancer.

Liechty *et al.* (1998) analyzed a large number of spontaneous *Tk* mutants using LOH analysis as well as chromosome painting. Their analysis provided evidence to support the hypothesis that the MLA detects recombination. However, the mutants they analyzed were all spontaneous

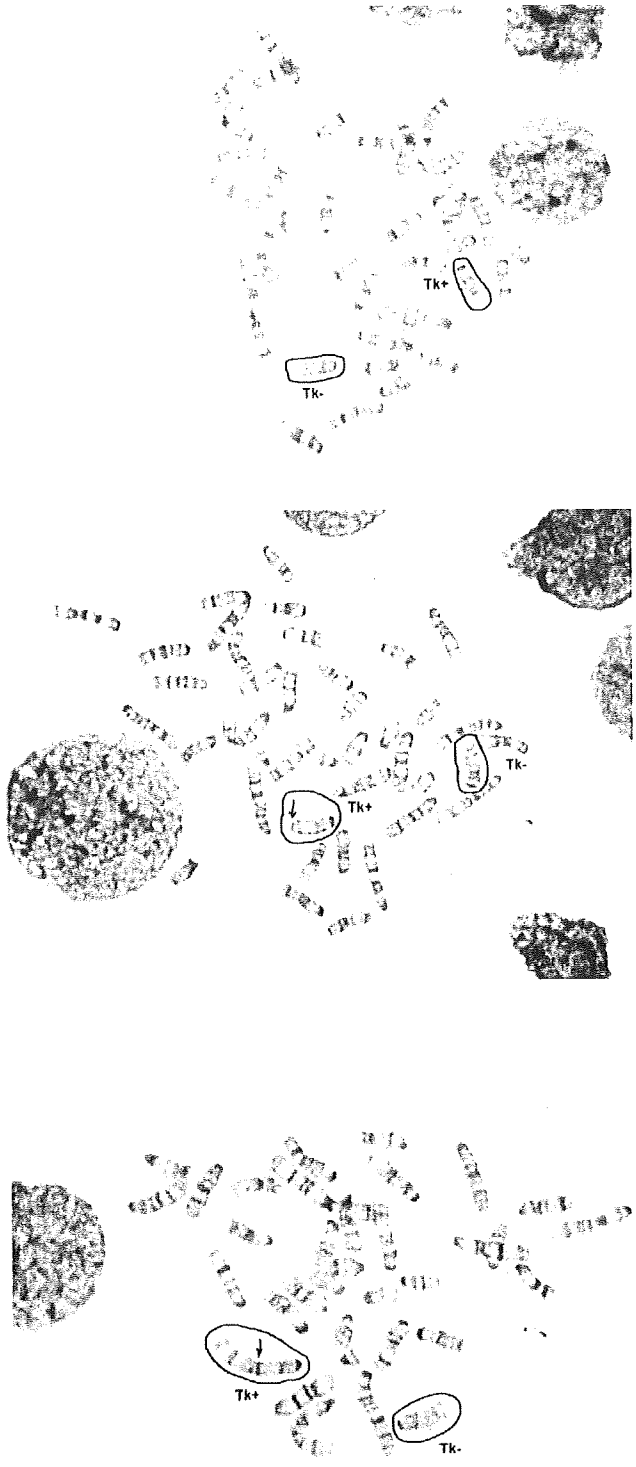

FIG. 2. G-banding analysis of mouse lymphoma *Tk* mutants A3C2, A6C2, and A5D6 that were isolated from a culture treated with 1 mg/ml AZT. The circled chromosomes are chromosome 11. The analysis of mutant A3C2 (top photo) shows a normal metaphase: two chromosome 11 with normal length and banding patterns (Tk^+ chromosome is on the right). The analysis of mutant A6C2 (middle photo) shows a visible deletion of the Tk^+ chromosome (left, indicated by an arrow). The Tk^- chromosome (right) has a normal banding pattern. The analysis of mutant A5D6 (bottom photo) shows a visible deletion of the distal Tk^+ chromosome resulting from an unbalanced translocation (translocation site indicated by an arrow). The Tk^- chromosome (right) has a normal banding pattern. Note that the Tk^+ chromosome has a bigger centromere than the Tk^- chromosome. This centromeric heteromorphism can be used to distinguish between the Tk^+ and Tk^- chromosomes.

FIG. 3. G-banding analysis of mouse lymphoma *Tk* mutants MS8 (isolated from a cell culture treated with 0.4 μg/ml mitomycin C) and mutant A5D2 (isolated from a cell culture treated with 1 mg/ml AZT). Their metaphase cells display complex chromosome alterations. The circled chromosomes are chromosome 11. The Tk^+ chromosome has a bigger centromere than the Tk^- chromosome. This centromeric heteromorphism can be used to distinguish between the Tk^+ and Tk^- chromosomes. In the top photo for mutant MS8, the Tk^- chromosome (top) shows a normal banding pattern, while the Tk^+ chromosome (bottom) is abnormally long. It is formed by two chromosome 11 joined together (translocation site indicated by an arrow). In the bottom photo for mutant A5D2, two Tk^- chromosomes were identified: one (left) shows a normal banding pattern; the other (middle) is translocated to another chromosome (translocation site indicated by an arrow). The Tk^+ chromosome (right) was partially deleted by an unbalanced translocation (translocation site indicated by an arrow).

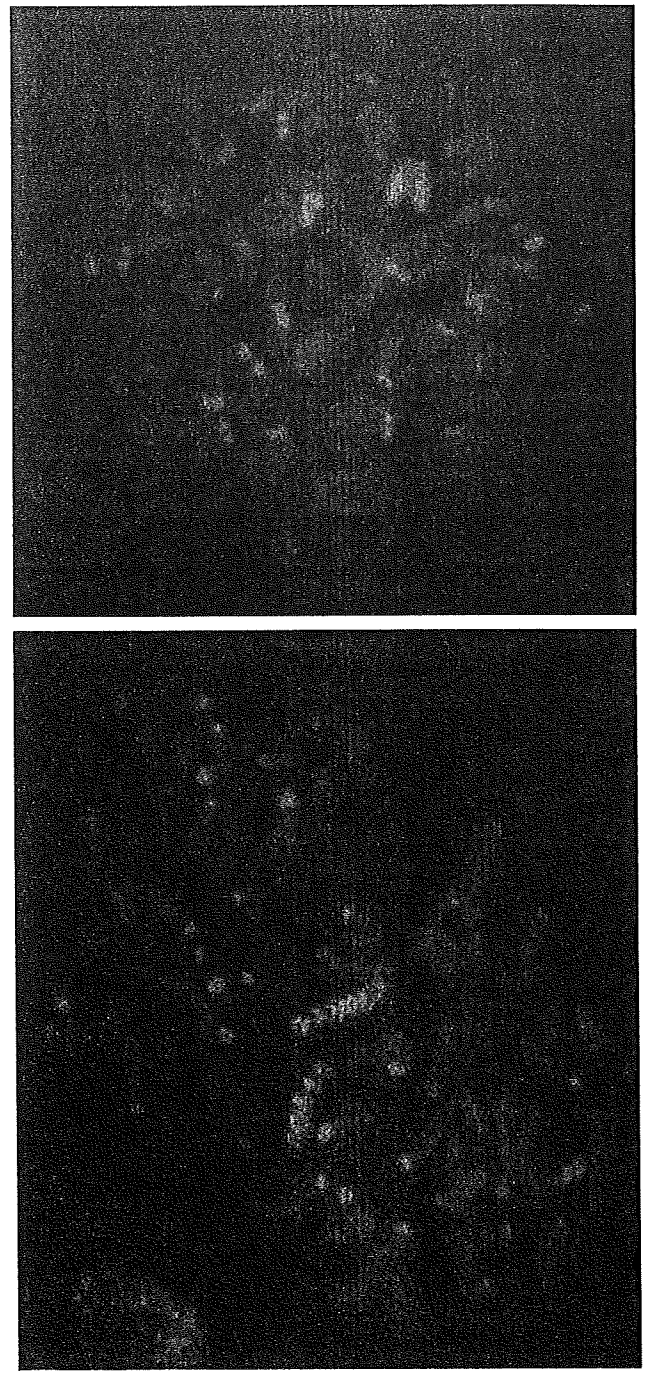

FIG. 4. Chromosome painting analysis of mouse lymphoma *Tk* mutants TL8 and TL2 that were isolated from a culture treated with 1 μg/ml taxol. The chromosome 11 probe is labeled with red fluorescence. The top photo for mutant TL8 shows only one chromosome 11 (chromosome loss). The bottom photo for mutant TL2 shows two chromosome 11 (chromosome duplication after loss).

mutants. In addition, although chromosome painting is relatively easy to perform and analyze, it is not as informative as conventional G-banding analysis. In their study, four mutants showed interesting chromosome alterations: two chromosome 11 with different lengths. Without G-banding analysis, those aberrations could not be identified. Previously we analyzed a mutant isolated from a bleomycin-treated culture (mutant 950, Clark *et al.*, 2004) and chromosome painting showed a similar result: two chromosome 11 with different lengths, with a partial LOH pattern. This was first interpreted as a deletion. However, further analysis using G-banding revealed

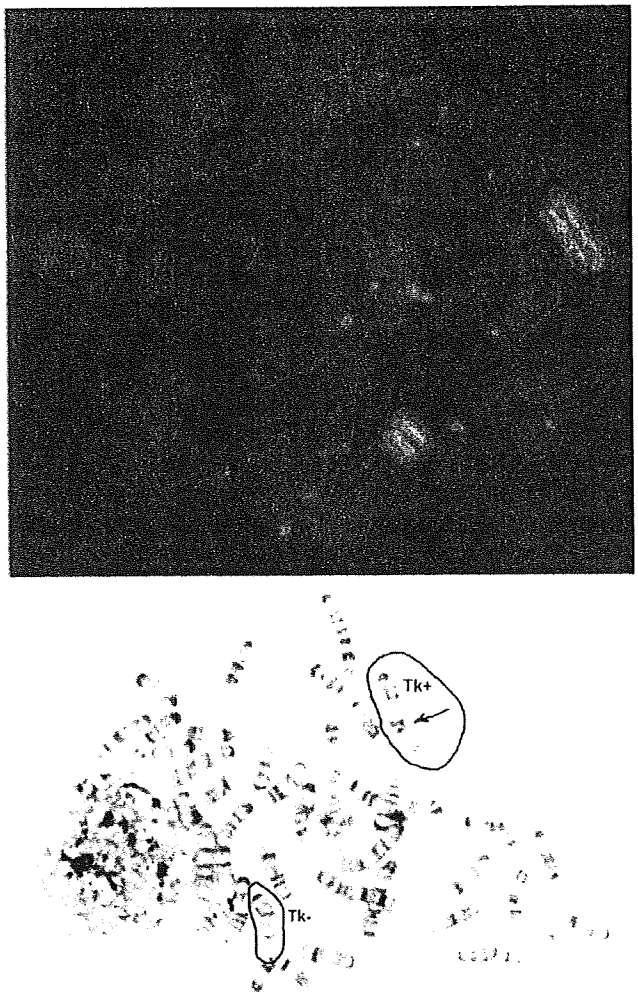

FIG. 5. Chromosome painting and G-banding analysis of mouse lymphoma *Tk* mutant 950 isolated from a bleomycin-treated culture (Clark *et al.*, 2004). The chromosome 11 probe is labeled with red fluorescence. Chromosome painting (top photo) shows two chromosome 11 of different length. The G-banding analysis (bottom photo) shows complex chromosome alterations. The circled chromosomes are chromosome 11. The Tk^- chromosome (left) shows a normal banding pattern, while the Tk^+ chromosome (right) is abnormally long. It is formed by two chromosome 11 joined together (translocation site indicated by an arrow). Note that the Tk^+ chromosome has a bigger centromere than the Tk^- chromosome. This centromeric heteromorphism can be used to distinguish between the Tk^+ and Tk^- chromosomes.

that the "longer" chromosome 11 was actually formed by two (or two parts of) chromosome 11 in an unbalanced translocation, while the "shorter" chromosome 11 was actually a normal Tk^- chromosome (Fig. 5). Therefore, in this study we used a combination of all the different analysis methods to identify the mutation types. Interestingly, five mutants (four from the AZT treatment and one from mitomycin C) were found to have alterations similar to mutant 950: deletion with aneuploidy. The proportion of this specific aberration in the mutants we analyzed is very high: 5 of the 19 analyzed were partial chromosome 11 LOH mutants. The underlying mechanism for this event is unclear. We speculate that the Tk^- chromosome duplication is some type of compensation for the deletion of the Tk^+ chromosome, resulting in partial trisomy (aneuploidy). This unique aberration may be related to the clastogenicity of the chemical: AZT, mitomycin C, and bleomycin are all clastogens.

Although chromosome loss is the primary mutation mechanism whereby aneugens induce Tk^--deficient mutants, few cells were found to be monosomic for chromosome 11 in this study. We analyzed nine mutants showing complete chromosome 11 LOH. The majority were mosaic with most having chromosome duplication after loss. This probably occurs because duplication of the Tk^- chromosome is a repair/compensation mechanism after the loss of the Tk^+ chromosome. Cells containing two Tk^- chromosomes would be expected to have a growth advantage over cells containing only one Tk^- chromosome, thereby becoming the predominant cell type in the culture (Honma *et al.*, 2001).

The results clearly demonstrate that MLA *Tk* mutants can result from recombination, deletion, and aneuploidy. The ability to detect recombination is a particular advantage of the MLA. Recombination is an important pathway for repairing DNA double-strand breaks, and it is essential for cellular survival in mammals (Helleday, 2003). It cannot be detected by assays using hemizygous reporter genes, such as *Hprt*. The ability to detect large deletions is another advantage of the MLA. This may be due to the *Trp53* status of the L5178Y/$Tk^{+/-}$ mouse lymphoma cell line. In this cell line, both alleles of the *Trp53* gene have point mutations, one of which likely results in no protein production (the point mutation produces a stop codon) and the other results in the production of a mutant Trp53 (Clark *et al.*, 1998; Storer *et al.*, 1997). Large-scale damage may be incompatible with the survival of Trp53-sufficient cells; these cells will undergo apoptosis under the surveillance of Trp53 (Honma *et al.*, 2000). The Trp53 status may also play a critical role in the ability of the MLA to detect aneuploidy (Honma *et al.*, 2001). In mammalian cells, Trp53 is involved in the maintenance of diploidy by participating in a mitotic checkpoint and the regulation of centrosome duplication (Cross *et al.*, 1995; Honma *et al.*, 2001; Tarapore and Fukasawa, 2000).

It should be emphasized that while this analysis indicates that the MLA can detect newly induced deletions, mitotic recombination, and aneuploidy, it does not provide insight into the relative proportion of the various types of mutational events or the efficiency with which these events are detected. While we have combined several powerful techniques to elucidate the mutations, all these techniques are very "blunt" tools. The nine LOH markers were distributed across chromosome 11, but from the perspective of potentially mutable sites, only a tiny fraction of the chromosome could be evaluated. Furthermore, our strategy of combining the G-banding analysis with the LOH analysis to distinguish between deletion and mitotic recombination required that the breakpoints be located so that at least approximately 25%

of the chromosome would be deleted (and readily visible by banded karyotype) if the mutant were a deletion rather than resulting from mitotic recombination.

To understand the mechanism for the induction of every mutant, and ultimately to fully understand the fundamental differences between the small and LC *Tk* mutants, the analysis must be conducted in a way that can interrogate a much larger portion of chromosome 11. We are currently initiating a research project to utilize comparative genomic hybridization microarray technology in combination with our current tools.

Our present study clearly demonstrates that the MLA can, in fact, detect deletion, recombination, and aneuploidy and provides new evidence for the utility of the MLA in a mechanistically based genotoxicity hazard identification battery. Depending upon the question that is being addressed and the importance of understanding the mutations induced by a particular chemical, our strategy of combining cytogenetic and molecular analysis of mutants can be used to provide more than a simple mutagenic/nonmutagenic hazard assessment.

FUNDING

Supported in part by an appointment (J.W.) to the Research Participation Program at the National Center for Toxicological Research administered by the Oak Ridge Institute of Science and Education (Oak Ridge, TN) through an interagency agreement between the U.S. Department of Energy and the U.S. Food and Drug Administration

ACKNOWLEDGMENTS

Disclaimer: The findings and conclusions in this report are those of the authors and do not necessarily represent the views of the U.S. Food and Drug Administration.

REFERENCES

Aardema, M. J., Albertini, S., Arni, P., Henderson, L. M., Kirsch-Volders, M., Mackay, J. M., Sarrif, A. M., Stringer, D. A., and Taalman, R. D. F. (1998). Aneuploidy: A report of an ECETOC task force. *Mutat. Res.* **410,** 3–79.

Applegate, M. L., Moore, M. M., Broder, C. B., Burrell, A., Juhn, G., Kasweck, K. L., Lin, P. F., Wadhams, A., and Hozier, J. C. (1990). Molecular dissection of mutations at the heterozygous thymidine kinase locus in mouse lymphoma cells. *Proc. Natl Acad. Sci. U.S.A.* **87,** 51–55.

Blazak, W. F., Los, F. J., Rudd, C. J., and Caspary, W. J. (1989). Chromosome analysis of small and large L5178Y mouse lymphoma cell colonies: Comparison of trifluorothymidine-resistant and unselected cell colonies from mutagen-treated and control cultures. *Mutat. Res.* **224,** 197–208.

Blazak, W. F., Stewart, B. E., Galperin, I., Allen, K. L., Rudd, C. J., Mitchell, A. D., and Caspary, W. J. (1986). Chromosome analysis of trifluorothymidine-resistant L5178Y mouse lymphoma cell colonies. *Environ. Mutagen.* **8,** 229–240.

Chen, T., Harrington-Brock, K., and Moore, M. M. (2002). Mutant frequencies and loss of heterozygosity induced by N-ethyl-N-nitrosourea (ENU) in the thymidine kinase (*TK*) gene of L5178Y/$Tk^{+/-}$-3.7.2C mouse lymphoma cells. *Mutagenesis* **17,** 105–109.

Chen, T., and Moore, M. M. (2004). Screening for chemical mutagens using the Mouse Lymphoma Assay. In *Methods in Pharmacology and Toxicology Optimization in Drug Discovery: In Vitro Methods* (Z. Yan and G. W. Caldwell, Eds.), pp. 337–352. Humana Press, Totowa, NJ.

Cimino, M. C., Tice, R. R., and Liang, J. C. (1986). Aneuploidy in mammalian somatic cells *in vivo*. *Mutat. Res.* **167,** 107–122.

Clark, L. S., Harrington-Brock, K., Wang, J., Sargent, L., Lowry, D., Reynolds, S. H., and Moore, M. M. (2004). Loss of P53 heterozygosity is not responsible for the small colony thymidine kinase mutant phenotype in L5178Y mouse lymphoma cells. *Mutagenesis* **19,** 263–268.

Clark, L. S., Hart, D. W., Vojta, P. J., Harrington-Brock, K., Barrett, J. C., Moore, M. M., and Tindall, K. R. (1998). Identification and chromosomal assignment of two heterozygous mutations in the *Trp53* gene in L5178Y $Tk^{+/-}$ 3.7.2C mouse lymphoma cells. *Mutagenesis* **13,** 427–434.

Clive, D., Glover, P., Applegate, M., and Hozier, J. (1990). Molecular aspects of chemical mutagenesis in L5178Y/$Tk^{+/-}$ mouse lymphoma cells. *Mutagenesis* **5,** 191–197.

Cross, S. M., Sanchez, C. A., Morgan, C. A., Schimke, M. K., Ramel, S., Idzerda, R. L., Raskind, W. H., and Reid, B. J. (1995). A p53-dependent mouse spindle checkpoint. *Science* **267,** 1353–1356.

Davies, M. J., Phillips, B. J., and Rumsby, P. C. (1993). Molecular analysis of mutations at the *Tk* locus of L5178 mouse lymphoma cells induced by ethyl methanesulphonate and mitomycin C. *Mutat. Res.* **290,** 145–153.

Dearfield, K. L., and Moore, M. M. (2005). Use of genetic toxicology information for risk assessment. *Environ. Mol. Mutagen.* **46,** 236–245.

Dobrovolsky, V. N., Shaddock, J. G., and Heflich, R. H. (2002). Mutagenicity of gamma-radiation, mitomycin C, and etoposide in the *Hprt* and *Tk* genes of $Tk^{+/-}$ mice. *Environ. Mol. Mutagen.* **39,** 342–347.

Duesberg, P., Rasnick, D., Li, R., Winters, L., Rausch, C., and Hehlmann, R. (1999). How aneuploidy may cause cancer and genetic instability. *Anticancer Res.* **19,** 4887–4906.

Helleday, T. (2003). Pathways for mitotic homologous recombination in mammalian cells. *Mutat. Res.* **532,** 103–115.

Honma, M., Hayashi, M., Shimada, H., Tanaka, N., Wakuri, S., Awogi, T., Yamamoto, K. I., Ushio-Kodani, K. N., Nishi, Y., Nakadate, M., *et al.* (1999). Evaluation of the mouse lymphoma *Tk* assay (microwell method) as an alternative to the *In vitro* chromosomal aberration test. *Mutagenesis* **14,** 5–22.

Honma, M., Momose, M., Sakamoto, H., Sofuni, T., and Hayashi, M. (2001). Spindle poisons induce allelic loss in mouse lymphoma cells through mitotic non-disjunction. *Mutat. Res.* **493,** 101–114.

Honma, M., Momose, M., Tanabe, H., Sakamoto, H., Yu, Y., Little, J. B., Sofuni, T., and Hayashi, M. (2000). Requirement of wild-type p53 protein for maintenance of chromosomal integrity. *Mol. Carcinog.* **28,** 203–214.

Hozier, J., Applegate, M., and Moore, M. M. (1992). *In vitro* mammalian mutagenesis as a model for genetic lesions in human cancer. *Mutat. Res.* **270,** 201–209.

Hozier, J., Sawyer, J., Clive, D., and Moore, M. M. (1982). Cytogenetic distinction between the TK^{+} and TK^{-} chromosomes in the L5178Y $TK^{+/-}$ 3.7.2C mouse-lymphoma cell line. *Mutat. Res.* **105,** 451–456.

Hozier, J., Sawyer, J., Moore, M., Howard, B., and Clive, D. (1981). Cytogenetic analysis of the L5178Y/$TK^{+/-}$ → $TK^{-/-}$ mouse lymphoma mutagenesis assay system. *Mutat. Res.* **84,** 169–181.

Ikui, A. E., Yang, C. P., Matsumoto, T., and Horwitz, S. B. (2005). Low concentrations of taxol cause mitotic delay followed by premature dissociation of p55CDC from Mad2 and BubR1 and abrogation of the spindle checkpoint, leading to aneuploidy. *Cell Cycle* **4,** 1385–1388.

Joseph, G., Grist, S., Firgaira, F., Turner, D., and Morley, A. (1993). Classification of mutations at the HLA-A locus by use of the polymerase chain reaction. *Environ. Mol. Mutagen.* **22,** 152–156.

Liechty, M. C., Crosby, H., Jr., Murthy, A., Davis, L. M., Caspary, W. J., and Hozier, J. C. (1996). Identification of a heteromorphic microsatellite within the thymidine kinase gene in L5178Y mouse lymphoma cells. *Mutat. Res.* **371,** 265–271.

Liechty, M. C., Hassanpour, Z., Hozier, J., and Clive, D. (1994). Use of microsatellite DNA polymorphisms on mouse chromosome 11 for *in vitro* analysis of thymidine kinase gene mutations. *Mutagenesis* **9,** 423–427.

Liechty, M. C., Scalzi, J. M., Sims, K. R., Crosby, H., Jr., Spencer, D. L., Davis, L. M., Caspary, W. J., and Hozier, J. C. (1998). Analysis of large and small colony L5178Y $Tk^{-/-}$ mouse lymphoma mutants by loss of heterozygosity (LOH) and by whole chromosome 11 painting: Detection of recombination. *Mutagenesis* **13,** 461–474.

Mailhes, J. B., Carabatsos, M. J., Young, D., London, S. N., Bell, M., and Albertini, D. F. (1999). Taxol-induced meiotic maturation delay, spindle defects, and aneuploidy in mouse oocytes and zygotes. *Mutat. Res.* **423,** 79–90.

Moore, M. M., Clive, D., Hozier, J. C., Howard, B. E., Batson, A. G., Turner, N. T., and Sawyer, J. R. (1985). Analysis of trifluorothymidine-resistant (TFTr) mutants of L5178Y/$TK^{+/-}$ mouse lymphoma cells. *Mutat. Res.* **151,** 161–174.

Moore, M. M., Mei, N., Chen, L., and Chen, T. (2005). Taxol induces mutations in the *Tk* gene of L5178Y/$Tk^{+/-}$ mouse lymphoma cells through a mitotic non-disjunction mechanism. *Toxicologist* **84,** 455.

Oshimura, M., and Barrett, J. C. (1986). Chemically-induced aneuploidy in mammalian cells: Mechanisms of biological significance in cancer. *Environ. Mol. Mutagen.* **8,** 129–159.

Sawyer, J. R., Moore, M. M., Clive, D., and Hozier, J. C. (1985). Cytogenetic characterization of the L5178Y $TK^{+/-}$ 3.7.2C mouse lymphoma cell line. *Mutat. Res.* **147,** 243–253.

Schiff, P. B., and Horwitz, S. B. (1980). Taxol stabilizes microtubules in mouse fibroblast cells. *Proc. Natl Acad. Sci. U.S.A.* **77,** 1561–1565.

Sen, S. (2000). Aneuploidy and cancer. *Curr. Opin. Oncol.* **12,** 82–88.

Storer, R. D., Kraynak, A. R., McKelvey, T. W., Elia, M. C., Goodrow, T. L., and DeLuca, J. G. (1997). The mouse lymphoma L5178Y $Tk^{+/-}$ cell line is heterozygous for a codon 170 mutation in the p53 tumor suppressor gene. *Mutat. Res.* **373,** 157–165.

Tarapore, P., and Fukasawa, K. (2000). *p53* mutation and mitotic infidelity. *Cancer Invest.* **18,** 148–155.

Wang, J., Chen, T., Honma, M., Chen, L., and Moore, M. M. (2007). 3′-azido-3′-deoxythymidine induces deletions in L5178Y mouse lymphoma cells. *Environ. Mol. Mutagen.* **48,** 248–257.

Zhang, L. S., Honma, M., Matsuoka, A., Suzuki, T., Sofuni, T., and Hayashi, M. (1996). Chromosome painting analysis of spontaneous and methyl methanesulfonate- induced trifluorothymidine-resistant L5178Y cell colonies. *Mutat. Res.* **370,** 181–190.

Environmental and Molecular Mutagenesis 50:815–822 (2009)

Research Article

Dependence of DNA Double Strand Break Repair Pathways on Cell Cycle Phase in Human Lymphoblastoid Cells

Yoshio Takashima, Mayumi Sakuraba, Tomoko Koizumi, Hiroko Sakamoto, Makoto Hayashi, and Masamitsu Honma*

Division of Genetics and Mutagenesis, National Institute of Health Sciences, 1-18-1 Kamiyoga, Setagaya-ku, Tokyo 158-8501, Japan

DNA double-strand breaks (DSBs) are usually repaired by nonhomologous end-joining (NHEJ) or homologous recombination (HR). NHEJ is thought to be the predominant pathway operating in mammalian cells functioning in all phases of the cell cycle, while HR works in the late-S and G2 phases. However, relative contribution, competition, and dependence on cell cycle phases are not fully understood. We previously developed a system to trace the fate of DSBs in the human genome by introducing the homing endonuclease I-SceI site into the thymidine kinase (*TK*) gene of human lymphoblastoid TK6 cells. Here, we use this system to investigate the relative contribution of HR and NHEJ for repairing I-SceI-induced DSBs under various conditions. We used a novel transfection system, Amaxa™ nucleofector, which directly introduces the I-SceI expression vector into cell nuclei. Approximately 65% of transfected cells expressed the I-SceI enzyme and over 50% of the cells produced a single DSB in the genome. The relative contribution of NHEJ and HR for repairing the DSB was ~100:1 and did not change with transfection efficiency. Cotransfection with KU80-siRNA significantly diminished KU80 protein levels and decreased NHEJ activity, but did not increase HR. We also investigated HR and NHEJ in synchronized cells. The HR frequency was 2–3 times higher in late-S/G2 phases than in G1, whereas NHEJ was unaffected. Even in late-S/G2 phases, NHEJ remained elevated relative to HR. Therefore, NHEJ is the major pathway for repairing endonuclease-induced DSBs in mammalian cells even in late-S/G2 phase, and does not compete with HR. Environ. Mol. Mutagen. 50:815–822, 2009.

Key words: double strand breaks (DSBs); I-SceI site; non-homologous end joining (NHEJ); homologous recombination (HR); human cells

INTRODUCTION

Chromosomal double-strand breaks (DSBs) can be caused by ionizing radiation, chemicals, or endogenous processes that include V(D)J recombination and meiotic exchange. If these lesions are not repaired or are misrepaired, they can result in genomic rearrangement or cell death. The repair of DSBs is therefore essential for the maintenance of genomic integrity [Olive, 1998; van Gent et al., 2001]. The two major pathways responsible for such repair are homologous recombination (HR) and nonhomologous end joining (NHEJ) [Haber, 2000; Jackson, 2002]. As HR repairs DSBs using the undamaged homologous sequence as a template, we hypothesize that HR would take place mainly in the late-S and G2 phases of the cell cycle, when sister chromatids are available as templates. NHEJ, in contrast, should operate in all cell cycle phases. Many studies examining the relative contribution of NHEJ and HR in the repair of ionizing radiation-induced DSBs, demonstrate that their contribution varies with cell cycle phase [Takata et al., 1998; Rothkamm et al., 2003]. Ionizing radiation, however, produces not only DSBs but also single-strand breaks, various kinds of base and sugar damage, DNA interstrand crosslinks, and DNA-protein crosslinks [Brenner and Ward, 1992].

"Yoshio Takashima is currently at Research Center for Radiation Emergency Medicine, National Institute of Radiological Sciences, 4-9-1 Anagawa, Inage-ku, Chiba-shi, 263-8555, Japan."

*Correspondence to: Masamitsu Honma, Division of Genetics and Mutagenesis, National Institute of Health Sciences, 1-18-1 Kamiyoga, Setagaya-ku, Tokyo 158-8501, Japan. E-mail: honma@nihs.go.jp

Received 25 November 2008; provisionally accepted 18 January 2009; and in final form 19 January 2009

DOI 10.1002/em.20481

Published online 28 April 2009 in Wiley InterScience (www.interscience.wiley.com).

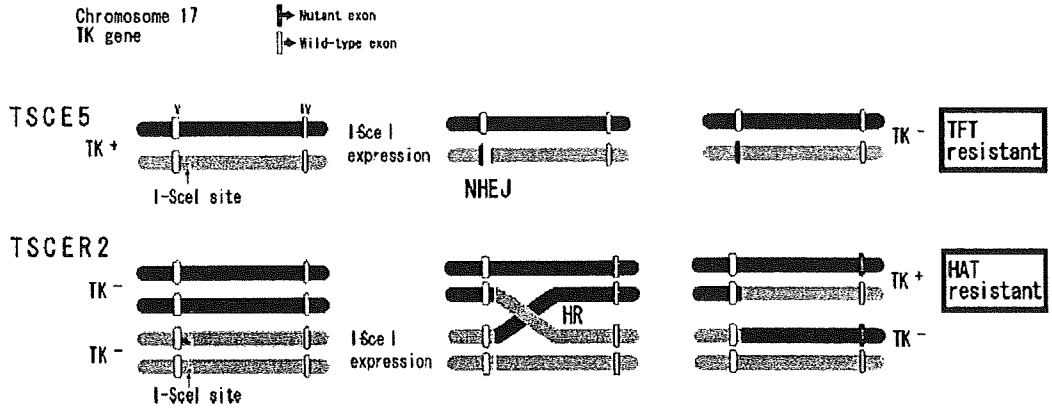

Fig. 1. Detection of NHEJ and HR in TSCE5 and TRSCR2 cells, respectively. Closed and shadowed bars represent mutant and wild-type alleles. In TSCE5, when a DSB at the I-*Sce*I site is repaired by NHEJ, a deletion results in exon 5, and TK-deficient mutants can be isolated in TFT medium. In TSCER2, when HR repairs the DSB, TK-proficient revertants are generated. The revertants can be selected in HAT medium.

Therefore, ionizing radiation-induced damage may not be ideal for the study of DSB repair. Recently, an understanding of DSB repair has emerged from systems that use the rare cutting restriction endonuclease from *Saccharomyces cerevisiae*, I-SceI [Johnson and Jasin, 2001]. Because the 18-bp recognition sequence of the I-*Sce*I gene is not present in most mammalian genomes and can be introduced by transfection, it is possible to generate site-specific DSBs in a mammalian chromosome or plasmid by expressing the I-SceI enzyme in genetically modified cells. This system was used to demonstrate that DSBs initiated HR and NHEJ of mammalian chromosomes. Most studies using this system, however, use artificial reporter substrates based on exogenous drug-resistance genes or a fluorescence gene, or are biased toward detecting specific deletion and recombination events [Sargent et al., 1997; Taghian and Nickoloff, 1997; Lin et al., 1999; Golding et al., 2004].

We previously developed a system to trace the fate of DSBs that occur in endogenous single-copy human genes [Honma et al., 2003, 2007]. Using gene-targeting, we introduced an I-*Sce*I site into the endogenous thymidine kinase (*TK*) gene of human lymphoblastoid TK6 cells, and developed cell lines that can detect NHEJ (TSCE5) and HR (TSCER2). TSCE5 is heterozygous (+/−) and TSCER2 is compound heterozygous (−/−) for the *TK* gene, and both have an I-*Sce*I site in intron 4. A DSB can be generated at the I-*Sce*I site by introducing I-SceI enzyme expression vector into the cells. NHEJ of the DSB results in TK-deficient mutants in TSCE5 cells, whereas HR between the alleles produces TK-proficient revertants in TSCER2 cells. The positive–negative drug selection assays for the TK phenotypes enable the distinction between NHEJ and HR events (Fig. 1). The assay system does not detect the genetic outcome of every NHEJ or HR event, because small deletion or small tract recombination that does not change the TK phenotype cannot be recovered. Furthermore, sister-chromatid recombination, which is also very important in HR, is also missed. Nonetheless, the system is very useful for understanding the role and mechanism of DSB repair in mammalian cells.

In the present study, we use the system described above to investigate the relative contribution of NHEJ and HR for repairing DSBs in TK6 cells. We also evaluate the dependence of both types of repair on cell cycle phases in synchronized cells. To understand the competition or cooperation between NHEJ and HR, we investigate repair activity in NHEJ knock-down cells generated by siRNA technology.

MATERIALS AND METHODS

Cell lines and Vectors

We used human lymphoblastoid cell lines TSCE5 and TSCER2, which are TK6 cells with an I-*Sce*I site inserted into the *TK* locus [Honma et al., 2003]. TSCE5 cells are heterozygous (*TK* +/−) for a point mutation in exon 4, and TSCER2 cells are compound heterozygous (*TK* −/−) for a point mutation in exons 4 and 5. NHEJ for a DSB occurring at the I-*Sce*I site results in TK-deficient mutants (*TK* −/−) in TSCE5 cells, while HR between the alleles produces TK-proficient revertants (TK +/−) in TSCER2 cells (Fig. 1). Cells were grown in RPMI 1640 medium (Gibco-BRL, Life technology, Grand Island, NY) supplemented with 10% heat-inactivated horse serum (JRH Biosciences, Lenexa, KS), 200 μg/ml sodium pyruvate, 100 U/ml penicillin, and 100 μg/ml streptomycin and maintained them at 10^5 to 10^6 cells/ml at 37°C in a 5% CO_2 atmosphere with 100% humidity.

The I-*Sce*I-expression vector, pCBASce, (kindly provided by Dr. Shunichi Takeda, Kyoto University) contains the coding sequences of the I-*Sce*I endonuclease from *Saccharomyces cerevisiae* under the control of the β-actin gene promoter [Fukushima et al., 2001]. We also constructed a pCBASce-off vector from pCBASce by inserting a 28-bp DNA fragment containing the 18-bp I-*Sce*I-restriction sequence between the 3′-end of its I-*Sce*I-nuclease coding sequence and a poly (A) site.

The expression of the I-SceI endonuclease of the pCBASce-off vector destroys the vector itself. Hence, its expression should be lost following transfection.

I-SceI Expression and Detection of NHEJ and HR

We electroporated ~5 × 10^6 cells using Amaxa™ nucleofector (Amaxa Biosystems, Gaithersburg, MD), program A-30, in solution V (provided by the supplier) with 50 μg/ml I-*SceI* expression vector, pCBASce or pCBASce-off. After 72 hr, cells were seeded into 96-well plates with trifluorothymidine (TFT) (for TK-mutants) or hypoxanthine, aminopterin, and thymidine (HAT) (for TK-revertants) medium. Drug resistant colonies were counted 2 weeks later.

Flow Cytometric and Microscopic Analysis with Immunofluorescence

We examined the post transfection kinetics of I-SceI expression using an anti-hemagglutinin A (HA) antibody [Guirouilh-Barbat et al., 2004] because the pCBASce vector coexpresses HA-tag together with I-SceI enzyme. Cells were fixed in 4% paraformaldehyde for 15 min at room temperature and permeabilized with 0.1% Triton X-100 (Sigma, St. Louis, MO) for 10 min. Immunofluorescence analysis was performed with an anti-HA antibody conjugated with Alexa Fluor 488 (Covance, Berkeley, CA), and transfection efficiency analyzed with an Epics XL flow cytometer (Beckman Coulter, Fullerton, CA) according to the manufacturer's recommendations.

Cells were also fixed with methanol on glass slides and immersed in PBS containing 0.5% Triton X100 for 30 min. To detect DSBs within individual cells, we conducted immunohistochemical analysis using gamma-H2AX antibody. The fixed cells were treated with a rabbit anti-phospho-gamma-H2AX antibody (Trevigen, Gaithersburg, MD), and then treated with a second antibody, goat Alexa Flour 488 anti-rabbit IgG (Invitrogen Japan KK, Tokyo, Japan).Cells were rinsed with PBS, stained with 4′,6-diamino-2-phenylindole dihydrochlorine (DAPI), and observed with a fluorescent microscope (Olympus, Tokyo, Japan).

siRNA and Western Blot Analysis

Cells were transfected with 50 nM KU80 small interfering RNA (siRNA; Santa Cruz Biotechnology, Santa Cruz, CA) using Amaxa™ nucleofector and Nucleofection Kit V. After 24-hr and 48-hr incubations, cell extracts were Western blotted using anti-KU86 (Santa Cruz Biotechnology) and anti-β-actin (Sigma) antibodies. Blots were exposed to horseradish peroxidase-labeled secondary antibodies (Amersham Pharmacia Biotech, Arlington Heights, IL), visualized using an enhanced chemiluminescence detection system, and quantified by densitometric scanning.

Cell Cycle Synchronization

A 2-step procedure was used to synchronize cells that included treatment with nocodazole (Sigma) followed by hydroxyurea (Sigma) because extended exposure to either chemical is genotoxic [Timson, 1975; Sun et al., 2005]. Cells were treated with 1 μM nocodazole for 12 hr followed by 2 mM hydroxyurea for 6 h to obtain a G1 rich cell population. Several hours later, following removal to a drug-free medium, the cell population shifted to the S/G2 phase. Cell cycle synchronization was established by flow cytometry. Cells were periodically harvested, washed in phosphate buffered saline (PBS), fixed in 70% cold ethanol, treated with 20 μg/ml RNase A (Wako Pure Chemical, Osaka, Japan), and stained with 10 μg/ml propidium iodide (Wako Pure Chemical). Approximately 10,000 cells per each sample were examined by EPICS-XL flow-cytometer (Beckman Coulter), and the data were quantitatively analyzed by MultiCycle AV software (Version. 4.0, Phoenix Flow Systems, San Diego, CA). A student's *t*-test was used to identify statistically significant differences in mutant frequencies.

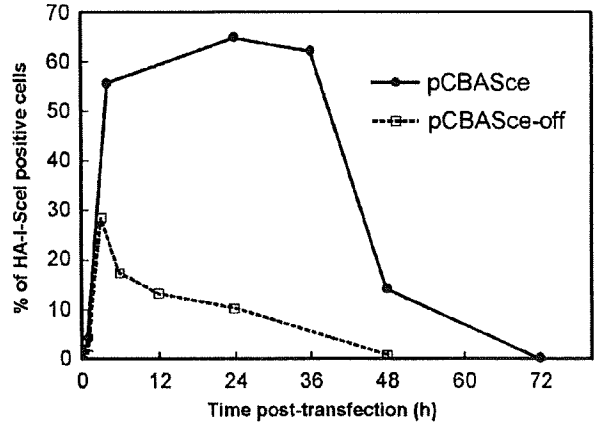

Fig. 2. Kinetics of I-*SceI* expression after transfection of pCBASce and pCBASce-off vectors. Detection of the anti-HA antibody tagged enzyme by flow cytometry.

RESULTS AND DISCUSSION

Expression of I-SceI and Generation of DSBs

The expression of the I-SceI enzyme in TSCE5 and TSCER2 cells generates a DSB in the *TK* gene. To introduce the expression vector into the cells, we used the Amaxa™ nucleofection system, which can directly transfer DNA into the nucleus at high efficiency [Honma et al., 2007]. We examined the kinetics of I-SceI expression by flow cytometry. The HA-tag attached to the I-SceI enzyme's amino terminus permits expression monitoring (Fig. 2). Expression was immediately apparent following introduction of pCBASce vector into TSCE5 cells. Twenty-four hours later, 65% of the cell population expressed the HA-tag. The expression continued to 48 hr, but not 72 hr. We also examined gamma-H2AX, a marker of DSBs [Fernandez-Capetillo et al., 2003; Nakamura et al., 2006]. Imunohistochemical analysis demonstrated that over 50% of the nucleofected cells showed a single DSB in their nuclei (Fig. 3). These results indicate that our I-SceI system with Amaxa™ nucleofection efficiently and specifically produced a DSB at the target site. The data also suggest that DSBs continue to occur up to at least 48 hr after nucleofection. Some DSBs may repeatedly occur and be repaired during that period, if an error-free pathway predominates [Honma et al., 2007].

We also developed a pCBASce-off vector based on pCBASce. This vector contains the 18 bp I-*SceI* restriction sequence between the 3′-end of I-*SceI*-nuclease coding sequence and the poly (A) site. The kinetics of

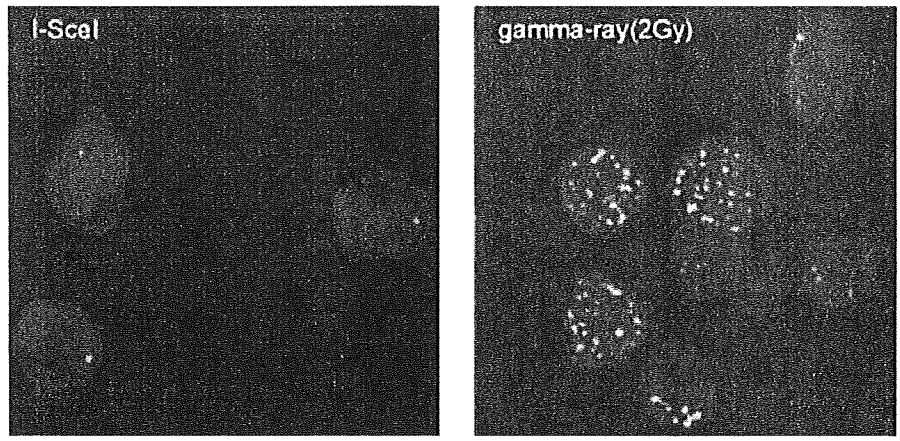

Fig. 3. Detection of DSBs by immunohistochemical analysis with gamma-H2AX antibody. Gamma-H2AX foci (green) in TSCE5 cells transfected with pCBASce vector (left) and cells irradiated with 2Gy gamma-ray (right). Nuclei were stained with DAPI. The transfection of pCBASce vector produced a single DSB in a TSCE5 cell at high efficiency.

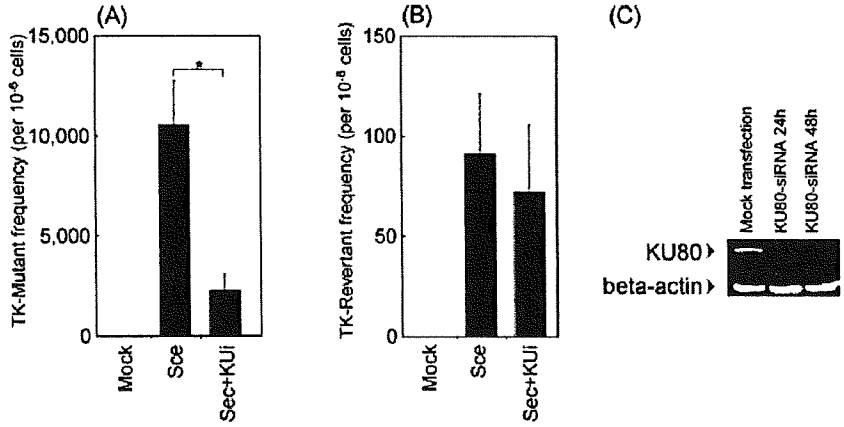

Fig. 4. Frequencies of TK-deficient mutants in TSCE5 (A) and TK-proficient revertants in TSCER2 (B). Mock-transfected control cells (Mock), cells transfected with the pCBASce vector (Sce), cells co-transfected with KU80 siRNA and the pCBASce vector (Sce+KU-i). The data are presented as the mean ± SD of 5 independent experiments; bars are SD. *$P < 0.05$. (C): Expression of KU80 protein. TSCE5 cells were transfected with KU80-siRNAs, and were conducted by Western blot analyses at 24 hr and 48 hr later after the transfection.

expression of the pCBASce-off vector is also shown in Figure 2. The expression of pCBASce-off vector reached a peak at 4 hr following transfection and immediately decreased. No expression was observed 48 hr later. This indicates that the pCBASce-off vector was destroyed by I-SceI-nuclease in the cells, and a DSB temporarily occurs in the *TK* gene. This may provide a more suitable model than DSBs caused by ionizing radiation, although the DSBs in the model do not correspond exactly with exogenous DSBs, and the DSB induction-efficiency is quite low. However, the model is useful to study cell-cycle dependent DNA repair and mutagenesis of DSBs.

NHEJ and HR for I-SceI-Induced DSBs in KU80-Competent and Knockdown Cells

Figures 4A and 4B show the frequency of the TK-deficient mutants in TSCE5 and TK-proficient revertants in TSCER2 cells. These mutants are the consequence of DSBs repaired by NHEJ and HR, respectively. The TK-deficient mutant frequency was 2.0×10^{-6} in the control TSCE5 cells. Introduction of the pCBASce vector elevated the frequency up to 1.1×10^{-2}, which was about 5,000 times higher than observed in control cells (Fig. 4A). The revertant frequency in TSCER2 also increased up to 0.9×10^{-4} following introduction of pCBASce

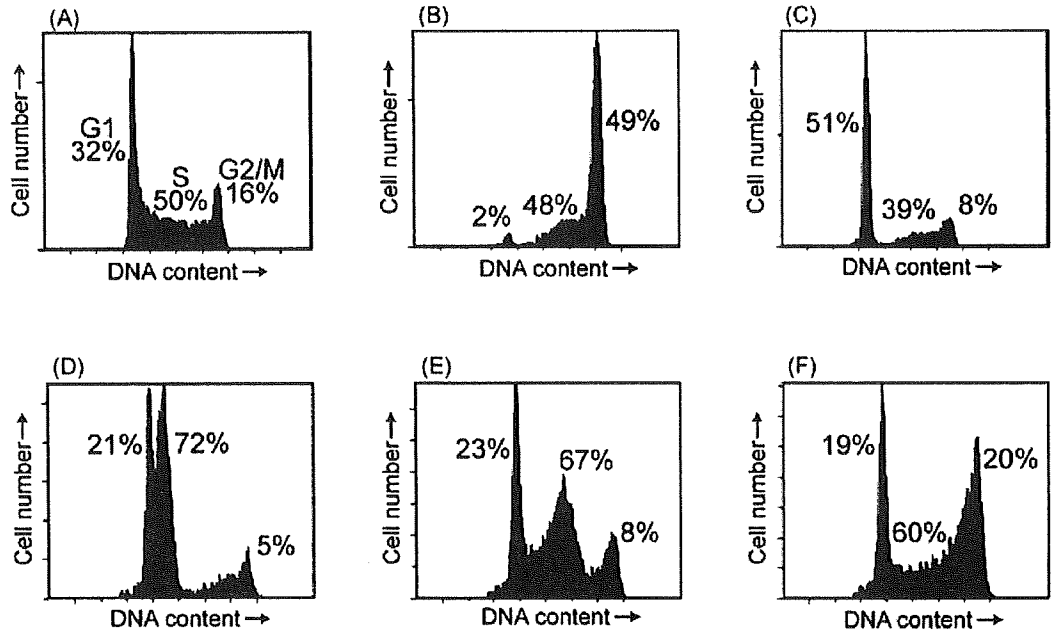

Fig. 5. DNA histograms for synchronization of cell cycle. Nonsynchronized cells (A) were arrested in the M phase with nocodazole (1 μM) for 12 hr, and (B) released into the media containing hydroxyurea (1 mM). After 6 hr incubation, the cells were arrested at the G1/S boundary (C), and released into a drug-free medium. The cells synchronously progressed through the cell cycle after being released from the hydroxyurea block (D–F). Cell cycle synchronization was confirmed by flow cytometry.

vector (Fig. 4B). These results suggest that the DSBs induced by the restriction enzyme are efficiently repaired by both NHEJ and HR. However, the relative contribution of NHEJ and HR was ~100:1, similar to our previous findings [Honma et al., 2007].

When TSCE5 and TSCER2 cells were transfected with the pCBASce-off vector, the TK-deficient mutant frequency was 1.6×10^{-3} in the TSCE5 cells, and the TK-revertant frequency was 1.3×10^{-5} in the TSCER2 cells. The lower frequency of mutants and revertants resulting from pCBASce-off relative to pCBASce is likely due to the low efficiency of expression of pCBASce-off (Fig. 2). However, the relative contribution of NHEJ and HR was not influenced.

Western blot analysis demonstrated that siRNA-mediated knockdown of KU80 proteins in the cells resulted in 94% and 75% reduction of KU protein at 24 hr and 48 hr after the transfection, respectively (Fig. 4C). TSCE5 cells that were cotransfected with the pCBASce vector and KU80 siRNA exhibited significantly lower NHEJ frequency (0.22×10^{-2}) than when the pCBASce vector alone was transfected (1.1×10^{-2}) (Fig. 4A). Conversely, HR frequency induced by DSBs in TSCER2 was not altered by KU80 knockdown (Fig. 4B). This suggests that NHEJ and HR do not simply compete for I-SceI induced DSBs [Delacote et al., 2002].

KU80 plays a major role in the NHEJ pathway for DSB repair in mammalian cells. It is believed that KU80 and KU70 bind to the DNA end, then recruit DNA-PKcs and stabilize their binding [Smith and Jackson, 1999; Lieber et al., 2003; Downs and Jackson, 2004]. A decrease in the TK-deficient mutant frequency following cotransfection with KU80 siRNA indicates that the TK-deficient mutants induced I-*Sce*I expression by NHEJ. However, NHEJ still predominantly repairs DSBs in the KU80-knockdown cells, which may reflect the activity of the remaining NHEJ by leaky KU80 protein or the presence of an alternative end-joining pathway [Iliakis et al., 2004; Lieber, 2008]. Schulte-Uentrop et al. suggested different genetic requirements for repairing I-SceI-induced DSBs because KU80 knock-out mouse cells did not lose end-joining activity for I-SceI-induced DSBs [Schulte-Uentrop et al., 2008]. Wu et al. proposed a backup NHEJ pathway (B-NHEJ) utilizing Ligase III and PARP-1 as an alternative to the classical DNA-PKcs dependent pathway (D-NHEJ) [Wu et al., 2008]. It was demonstrated that the efficiency of end-joining for restriction enzyme induced-DSBs was significantly suppressed in KU80 knock-out cells treated with PARP-1 inhibitors [Wang et al., 2006].

Contribution of NHEJ and HR in Repairing DSBs in Different Phases of the Cell Cycle

Cell cycles were synchronized using nocodasol (1 μM) and hydroxyurea (2 mM). Nonsynchronized cells (Fig. 5A) treated with nocodazole for 12 hr were arrested in M

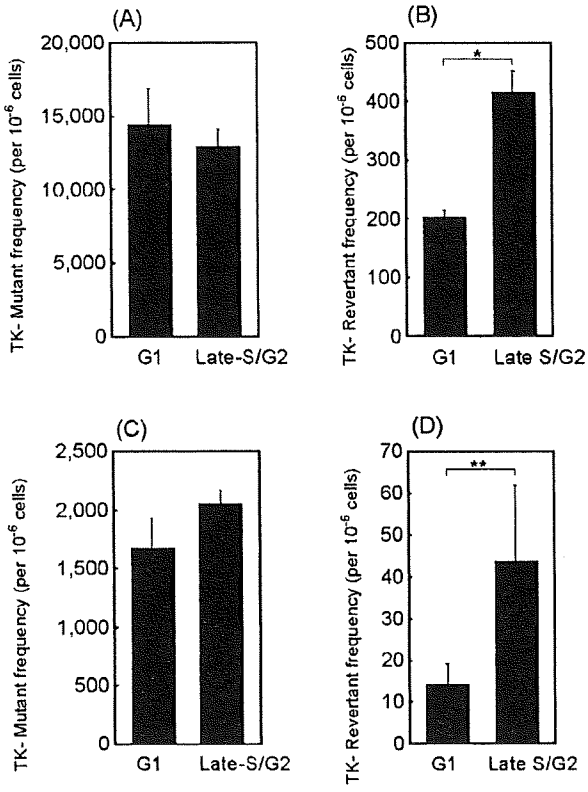

Fig. 6. Frequencies of TK-deficient mutants in synchronized TSCE5 cells (A, C) and of the TK-proficient revertants in synchronized TSCER2 cells. (A, C). The synchronized cells were transfected with pCBASce vector (A, B) and with pCBASce-off vector (C, D). The data are presented as the mean ± SD of three independent experiments; bars are SD. $*P < 0.05$, $**P < 0.1$.

phase (Fig. 5B) and released into the media containing hydroxylurea. After 6 hr incubation in hydroxyurea, cells were arrested at the G1/S boundary (Fig. 5C). The cells synchronously progressed through the cell cycle after being released from the hydroxyurea block (Figs. 5D–5F). Because I-SceI expression began 3 hr post transfection (Fig. 2), we transfected pCBASce vector into the cells at the M/G1 boundary (1 hr after release from the nocodazole block), and in early-S phase (1 hr after release from the hydroxyurea block) to efficiently generate DSBs at the G1 phase and the late-S/G2 phase, respectively. The cell populations at 3 hr following the transfection were as expected as shown in Figures 5D (G1) and 5E (late-S/G2).

The NHEJ frequency in the TSCE5 cells was 1.4×10^{-2} in the G1 phase and 1.3×10^{-2} in the late-S/G2 phase (Fig. 6A). In the TSCER2 cells, the HR frequency was 2.0×10^{-4} in the G1 phase and 4.1×10^{-4} in the late-S/G2 phase (Fig. 6B). Treatment with nocodazole and hydroxyurea did not affect colony-forming efficiency (data not shown). The HR frequency was twofold higher in late-S/G2 cells than in G1 cells, whereas the frequency of NHEJ was not dependent on cell-cycle phase. We also transfected the pCBASce-off vector into the synchronized cells (Figs. 6C and 6D). Because the pCBASce-off vector is only briefly expressed following transfection, analysis of cell cycle dependence should be clear. Although no difference was observed for NHEJ frequencies between G1 (1.7×10^{-3}) and late-S/G2 (2.0×10^{-3}) phases (Fig. 6C), the HR frequency in the late-S/G2 cells (4.3×10^{-5}) was threefold higher than in the G1 cells (1.4×10^{-5}) (Fig. 6D). These results suggest that HR function is dependent on cell cycle, and is more active in the late-S/G2 phase.

The contribution of NHEJ and HR to the repair of DSBs in mammalian cells varies with the systems used to detect them [Rothkamm et al., 2003; Mao et al., 2008a]. In the present work, we demonstrated that NHEJ is equally functional in all cell cycle phases, whereas HR operates 2–3 times more efficiently in late-S/G2 than in G1. Because we could not completely synchronize the cell population, and could not perfectly introduce a DSB into the specific cell population even by using pCBASce-off vector, quantitative analysis for cell-cycle dependence of DSB repair is difficult. Saleh-Gohari and Helleday demonstrated that by using synchronized human cells containing a stably integrated copy of a recombination reporter gene, the frequency of HR repair of DSBs was 24-fold higher in S-phase cells than in G1/G0 cells [Saleh-Gohari and Helleday, 2004]. However, they did not examine the relative contributions of NHEJ and HR throughout the cell cycle phases. Recently, Mao et al. measured the efficiency of NHEJ and HR at different cell cycle stages in hTERT-immortalized diploid human fibroblast cells. They showed that the overall efficiency of NHEJ was higher than HR at all cell cycle stages, although HR works more efficiently in the S-phase [Mao et al., 2008b].

The conclusions of the present work support those described above. We demonstrate that NHEJ is the predominant mechanism for DSB repair even in late-S/G2 phase. Our systems, however, are unable to detect sister-chromatid recombination (SCR), which must be an important recombination event during late-S/G2 phase [Helleday, 2003]. Because SCR is an error-free pathway and does not leave any genetic change in principle, it is impossible to quantitatively measure SCR at the molecular level. Most systems for studying HR are designed to detect unusual SCR events that occur in artificial recombination substrates [Bertrand et al., 1997; Boehden et al., 2003; Richardson et al., 2004]. Because the I-SceI enzyme during the late-S/G2 phase cleaves both sister-chromatids, SCR may not occur in our system. Occasionally, if one of two sister-chromatids are broken, SCR may arise. If SCR predominantly works during late-S/G2 phase, NHEJ frequency must be suppressed. The lack of

change in NHEJ frequency across all phases of the cell cycle implies that NHEJ is the major DSB repair pathway and does not compete with HR. HR may be involved in a more prolonged attempt to repair persistent DNA lesions [Delacote et al., 2002; Frank-Vaillant and Marcand, 2002; Kim et al., 2005]. While I-SceI induced a single DSB, ionizing radiation and chemicals induce many different types of DNA damage [Nikjoo et al., 1997]. DSBs also endogenously arise by replication fork stalling or collapse during S phase [Delacote and Lopez, 2008; Llorente et al., 2008]. These lesions are thought to be repaired by strand invasion into a homologous duplex DNA followed by replication or HR [Llorente et al., 2008]. Therefore, the relative contribution of NHEJ and HR to DSB repair varies with the character of the lesion and the number of DSBs induced in the genome.

REFERENCES

Bertrand P, Rouillard D, Boulet A, Levalois C, Soussi T, Lopez BS. 1997. Increase of spontaneous intrachromosomal homologous recombination in mammalian cells expressing a mutant p53 protein. Oncogene 14:1117–1122.

Boehden GS, Akyuz N, Roemer K, Wiesmuller L. 2003. p53 mutated in the transactivation domain retains regulatory functions in homology-directed double-strand break repair. Oncogene 22:4111–4117.

Brenner DJ, Ward JF. 1992. Constraints on energy deposition and target size of multiply damaged sites associated with DNA double-strand breaks. Int J Radiat Biol 61:737–748.

Delacote F, Lopez BS. 2008. Importance of the cell cycle phase for the choice of the appropriate DSB repair pathway, for genome stability maintenance: The trans-S double-strand break repair model. Cell Cycle 7:33–38.

Delacote F, Han M, Stamato TD, Jasin M, Lopez BS. 2002. An xrcc4 defect or Wortmannin stimulates homologous recombination specifically induced by double-strand breaks in mammalian cells. Nucleic Acids Res 30:3454–3463.

Downs JA, Jackson SP. 2004. A means to a DNA end: The many roles of Ku. Nat Rev Mol Cell Biol 5:367–378.

Fernandez-Capetillo O, Celeste A, Nussenzweig A. 2003. Focusing on foci: H2AX and the recruitment of DNA-damage response factors. Cell Cycle 2:426–427.

Frank-Vaillant M, Marcand S. 2002. Transient stability of DNA ends allows nonhomologous end joining to precede homologous recombination. Mol Cell 10:1189–1199.

Fukushima T, Takata M, Morrison C, Araki R, Fujimori A, Abe M, Tatsumi K, Jasin M, Dhar PK, Sonoda E, Chiba T, Takeda S. 2001. Genetic analysis of the DNA-dependent protein kinase reveals an inhibitory role of Ku in late S-G2 phase DNA double-strand break repair. J Biol Chem 276:44413–44418.

Golding SE, Rosenberg E, Khalil A, McEwen A, Holmes M, Neill S, Povirk LF, Valerie K. 2004. Double strand break repair by homologous recombination is regulated by cell cycle-independent signaling via ATM in human glioma cells. J Biol Chem 279: 15402–15410.

Guirouilh-Barbat J, Huck S, Bertrand P, Pirzio L, Desmaze C, Sabatier L, Lopez BS. 2004. Impact of the KU80 pathway on NHEJ-induced genome rearrangements in mammalian cells. Mol Cell 14:611–623.

Haber JE. 2000. Partners and pathwaysrepairing a double-strand break. Trends Genet 16:259–264.

Helleday T. 2003. Pathways for mitotic homologous recombination in mammalian cells. Mutat Res 532:103–115.

Honma M, Izumi M, Sakuraba M, Tadokoro S, Sakamoto H, Wang W, Yatagai F, Hayashi M. 2003. Deletion, rearrangement, and gene conversion; genetic consequences of chromosomal double-strand breaks in human cells. Environ Mol Mutagen 42:288–298.

Honma M, Sakuraba M, Koizumi T, Takashima Y, Sakamoto H, Hayashi M. 2007. Non-homologous end-joining for repairing I-SceI-induced DNA double strand breaks in human cells. DNA Repair (Amst) 6:781–788.

Iliakis G, Wang H, Perrault AR, Boecker W, Rosidi B, Windhofer F, Wu W, Guan J, Terzoudi G, Pantelias G. 2004. Mechanisms of DNA double strand break repair and chromosome aberration formation. Cytogenet Genome Res 104:14–20.

Jackson SP. 2002. Sensing and repairing DNA double-strand breaks. Carcinogenesis 23:687–696.

Johnson RD, Jasin M. 2001. Double-strand-break-induced homologous recombination in mammalian cells. Biochem Soc Trans 29:196–201.

Kim JS, Krasieva TB, Kurumizaka H, Chen DJ, Taylor AM, Yokomori K. 2005. Independent and sequential recruitment of NHEJ and HR factors to DNA damage sites in mammalian cells. J Cell Biol 170:341–347.

Lieber MR. 2008. The mechanism of human nonhomologous DNA end joining. J Biol Chem 283:1–5.

Lieber MR, Ma Y, Pannicke U, Schwarz K. 2003. Mechanism and regulation of human non-homologous DNA end-joining. Nat Rev Mol Cell Biol 4:712–720.

Lin Y, Lukacsovich T, Waldman AS. 1999. Multiple pathways for repair of DNA double-strand breaks in mammalian chromosomes. Mol Cell Biol 19:8353–8360.

Llorente B, Smith CE, Symington LS. 2008. Break-induced replication: What is it and what is it for? Cell Cycle 7:859–864.

Mao Z, Bozzella M, Seluanov A, Gorbunova V. 2008a. Comparison of nonhomologous end joining and homologous recombination in human cells. DNA Repair (Amst) 7:1765–1771.

Mao Z, Bozzella M, Seluanov A, Gorbunova V. 2008b. DNA repair by nonhomologous end joining and homologous recombination during cell cycle in human cells. Cell Cycle 7:2902–2906.

Nakamura A, Sedelnikova OA, Redon C, Pilch DR, Sinogeeva NI, Shroff R, Lichten M, Bonner WM. 2006. Techniques for gamma-H2AX detection. Methods Enzymol 409:236–250.

Nikjoo H, O'Neill P, Goodhead DT, Terrissol M. 1997. Computational modelling of low-energy electron-induced DNA damage by early physical and chemical events. Int J Radiat Biol 71:467–483.

Olive PL. 1998. The role of DNA single- and double-strand breaks in cell killing by ionizing radiation. Radiat Res 150:S42–S51.

Richardson C, Stark JM, Ommundsen M, Jasin M. 2004. Rad51 overexpression promotes alternative double-strand break repair pathways and genome instability. Oncogene 23:546–553.

Rothkamm K, Kruger I, Thompson LH, Lobrich M. 2003. Pathways of DNA double-strand break repair during the mammalian cell cycle. Mol Cell Biol 23:5706–5715.

Saleh-Gohari N, Helleday T. 2004. Conservative homologous recombination preferentially repairs DNA double-strand breaks in the S phase of the cell cycle in human cells. Nucleic Acids Res 32: 3683–3688.

Sargent RG, Brenneman MA, Wilson JH. 1997. Repair of site-specific double-strand breaks in a mammalian chromosome by homologous and illegitimate recombination. Mol Cell Biol 17:267–277.

Schulte-Uentrop L, El Awady RA, Schliecker L, Willers H, Dahm-Daphi J. 2008. Distinct roles of XRCC4 and Ku80 in non-homologous end-joining of endonuclease- and ionizing radiation-induced DNA double-strand breaks. Nucleic Acids Res 36:2561–2569.

Smith GC, Jackson SP. 1999. The DNA-dependent protein kinase. Genes Dev 13:916–934.

Sun F, Betzendahl I, Pacchierotti F, Ranaldi R, Smitz J, Cortvrindt R, Eichenlaub-Ritter U. 2005. Aneuploidy in mouse metaphase II oocytes exposed in vivo and in vitro in preantral follicle culture to nocodazole. Mutagen 20:65–75.

Taghian DG, Nickoloff JA. 1997. Chromosomal double-strand breaks induce gene conversion at high frequency in mammalian cells. Mol Cell Biol 17:6386–6393.

Takata M, Sasaki MS, Sonoda E, Morrison C, Hashimoto M, Utsumi H, Yamaguchi-Iwai Y, Shinohara A, Takeda S. 1998. Homologous recombination and non-homologous end-joining pathways of DNA double-strand break repair have overlapping roles in the maintenance of chromosomal integrity in vertebrate cells. EMBO J 17:5497–5508.

Timson J. 1975. Hydroxyurea. Mutat Res 32:115–132.

van Gent DC, Hoeijmakers JH, Kanaar R. 2001. Chromosomal stability and the DNA double-stranded break connection. Nat Rev Genet 2:196–206.

Wang M, Wu W, Wu W, Rosidi B, Zhang L, Wang H, Iliakis G. 2006. PARP-1 and Ku compete for repair of DNA double strand breaks by distinct NHEJ pathways. Nucleic Acids Res 34:6170–6182.

Wu W, Wang M, Wu W, Singh SK, Mussfeldt T, Iliakis G. 2008. Repair of radiation induced DNA double strand breaks by backup NHEJ is enhanced in G2. DNA Repair (Amst) 7:329–338.

Accepted by—
C. Menck

Environmental and Molecular Mutagenesis 00:000–000 (2010)

Research Article

Genotoxicity of Acrylamide In Vitro: Acrylamide Is Not Metabolically Activated in Standard In Vitro Systems

Naoki Koyama,[1,2] Manabu Yasui,[1] Yoshimitsu Oda,[3] Satoshi Suzuki,[4] Tetsuo Satoh,[4] Takuya Suzuki,[5] Tomonari Matsuda,[5] Shuichi Masuda,[2] Naohide Kinae,[2] and Masamitsu Honma[1]*

[1]*Division of Genetics and Mutagenesis, National Institute of Health Sciences, 1-18-1 Kamiyoga, Setagaya-ku, Tokyo, Japan*
[2]*Laboratory of Food Hygiene, Graduate School of Food and Nutritional Sciences, University of Shizuoka, 52-1 Yada, Shizuaka-shi, Shizuoka, Japan*
[3]*Department of Applied Chemistry, Faculty of Science Engineering, Kinki University, 3-4-1, Kowakae, Higashiosaka-shi, Japan*
[4]*HAB Research Institute, Cornea Center Building, Ichikawa General Hospital, 5-11-13 Sugano, Ichikawa, Chiba, Japan*
[5]*Research Center for Environmental Quality Management, Kyoto University, 1-2 Yumihama, Otsu, Shiga, Japan*

The recent finding that acrylamide (AA), a genotoxic rodent carcinogen, is formed during the frying or baking of a variety of foods raises human health concerns. AA is known to be metabolized by cytochrome P450 2E1 (CYP2E1) to glycidamide (GA), which is responsible for AA's in vivo genotoxicity and probable carcinogenicity. In in-vitro mammalian cell tests, however, AA genotoxicity is not enhanced by rat liver S9 or a human liver microsomal fraction. In an attempt to demonstrate the in vitro expression of AA genotoxicity, we employed *Salmonella* strains and human cell lines that overexpress human CYP2E1. In the *umu* test, however, AA was not genotoxic in the CYP2E1-expressing *Salmonella* strain or its parental strain. Moreover, a transgenic human lymphoblastoid cell line overexpressing CYP2E1 (h2E1v2) and its parental cell line (AHH-1) both showed equally weak cytotoxic and genotoxic responses to high (>1 mM) AA concentrations. The DNA adduct N7-GA-Gua, which is detected in liver following AA treatment in vivo, was not substantially formed in the in vitro system. These results indicate that AA was not metabolically activated to GA in vitro. Thus, AA is not relevantly genotoxic in vitro, although its in vivo genotoxicity was clearly demonstrated. Environ. Mol. Mutagen. 00:000–000, 2010.

Key words: acrylamide; glycydamide; cytochrome P450 2E1 (CYP2E1), in vitro tests; *Salmonella*

INTRODUCTION

Recently, low levels of acrylamide (AA), a synthetic chemical widely used in industry, were detected in a variety of cooked foods [Tareke et al., 2000; Mottram et al., 2002]. It has been proposed that AA forms during frying and baking principally by the Maillard reaction between asparagine residues and glucose [Stadler et al., 2002; Tornqvist, 2005]. This finding raised concerns about a health risk for the general population [Tareke et al., 2002; Rice, 2005].

The International Agency for Research on Cancer classifies AA as 2A, a probable human carcinogen [IARC, 1994]. Because AA clearly induces gene mutations and micronuclei in mice, it could be a genotoxic carcinogen [Cao et al., 1993; Abramsson-Zetterberg, 2003; Manjanatha et al., 2005]. AA is metabolized by cytochrome P450 2E1 (CYP2E1) to glycidamide (GA), which can react with cellular DNA and protein [Sumner et al., 1999; Ghanayem et al., 2005a; Rice, 2005]. Two major GA-DNA adducts, N7-(2-carbamoyl-2-hydroxyethyl)-gua-

Grant sponsor: Health and Labor Sciences Research Grant, Japan; Grant Number: H21-food-general-012; Grant sponsor: Human Science Foundation, Japan; Grant Number: KHB1007.

*Correspondence to: Masamitsu Honma, Division of Genetics and Mutagenesis, National Institute of Health Sciences, 1-18-1 Kamiyoga, Setagaya-ku, Tokyo 158-8501, Japan. E-mail: honma@nihs.go.jp

Received 8 October 2009; provisionally accepted 5 January 2010; and in final form 19 January 2010

DOI 10.1002/em.20560

Published online in Wiley InterScience (www.interscience.wiley.com).

nine (N7-GA-Gua) and N3-(2-carbamoyl-2-hydroxyethyl)-adenine (N3-GA-Ade), have been identified in mice and rats treated with AA or GA [Segerback et al., 1995; Gamboa da Costa et al., 2003; Doerge et al., 2005], with the level of N7-GA-Gua being 100 times as high as the level of N3-GA-Ade in the test organ [Gamboa da Costa et al., 2003]. It is likely that these DNA adducts are responsible for AA's in vivo genotoxicity [Carere, 2006; Ghanayem and Hoffler, 2007]. In our previous study, however, AA did not induce micronuclei in human lymphoblastoid TK6 cells in the presence of rat liver S9, although the genotoxicity of *N*-di-*N*-butylnitrosamine (DBN), which is also metabolized by CYP2E1, was enhanced under the same conditions [Koyama et al., 2006]. Other in vitro genotoxicity studies have also failed to demonstrate the metabolic activation of AA in the presence of S9 [Knaap et al., 1988; Tsuda et al., 1993; Dearfield et al., 1995; Friedman, 2003]. It may be because most S9 preparations have low CYP2E1 activity [Calleman et al., 1990; Hargreaves et al., 1994].

In an attempt to demonstrate the genotoxicity of AA in vitro, we tested the compound using bacteria and mammalian cell lines that express CYP2E1. *S. typhimurium* OY1002/2E1 strain expresses respective human CYP2E1 enzyme and NADPH-cytochrome P450 reductase (reductase), and bacterial *O*-acetyltransferase [Oda et al., 2001]. Using the strain, as well as its parental strain not expressing these enzymes, we conducted an *umu* assay to evaluate induction of cytotoxicity and DNA damage by AA relative to that induced by its metabolite GA. The principle of the *umu* assay is based on the ability of the DNA-damaging agents inducing the *umu* operon. Monitoring the levels of *umu* operon expression enables us to quantitatively detect environmental mutagens [Oda et al., 1985]. In addition, we evaluated the relative mutagenicity of AA vs. GA in assays using transgenic human lymphoblastoid cell lines. Induction of gene mutation at the *TK* locus and of chromosome damage leading to micronucleus (MN) formation were assessed in the h2E1v2 which overexpress human CYP2E1 [Crespi et al., 1993a], vs. its parental cell line, AHH-1. We also investigated the relationship between AA genotoxicity and the formation N7-GA-Gua (derived from GA) in the in vitro mammalian cell system.

MATERIALS AND METHODS

Bacterial Strains, Cell Lines, Chemicals, and Human Liver Microsomal Fraction

For the bacterial tests, we used *umu* strain *S. typhimurium* OY1002/2E1, which expresses human CYP2E1, reductase, and bacterial *O*-acetyltransferase, and its parental strain, *S. typhimurium* TA1535/pSK1002 that does not express these enzymes [Oda et al., 2001].

For the mammalian cell tests, we used human lymphoblastoid cell lines, TK6, AHH-1, and h2E1v2. The TK6 cell line has been described previously [Honma et al., 1997]. The AHH-1 and h2E1v2 cell lines were kindly gifted from Dr. Charles Crespi (BD Bio Sciences, Bedford, MA). AHH-1 is a clonal isolate, derived from RPMI 1788 cells, which was selected for sensitivity to benzo[*a*]pyrene [Crespi and Thilly, 1984]. AHH-1 shows high activity of endogenous CYP1A1. Heterozygosity of AHH-1 cells at thymidine kinase (TK) locus was derived in a two-step selection process utilizing the frameshift mutagen, ICR-191. The AHH-1 cell line was then transfected with plasmids encoding human CYP2E1 enzymes, generating h2E1v2 cell line. AHH-1 expresses CYP1A1 and h2E1v2 expresses both CYP1A1 and CYP2E1 [Crespi et al., 1993a,b].

We purchased AA (CAS No. 79-06-1) and GA (CAS No. 5694-00-8) from Wako Pure Chemical (Tokyo) and dissolved them in phosphate-buffered saline just before use. We purchased *N*-di-*N*-methylnitorosamine (DMN) (CAS No. 62-75-9) from Sigma Aldrich Japan (Tokyo) and dissolved it in DMSO as a positive control for use. We purchased liver S9 prepared from SD rats treated with phenobarbital and 5,6-benzoflavone from the Oriental Yeast (Tokyo). The human liver S9 (HLS-104) was prepared from a human liver sample, which was legally procured from the NDRI (National Disease Research Interchange) in Philadelphia, USA, with permission to use for research purpose only. HLS-104 showed high activity of CYP2E1 [Hakura et al., 2005]. We prepared microsomal fraction from the S9 according to an established procedure [Suzuki et al., 2000]. We prepared the S9- or microsome-mix by mixing 4 ml S9 or microsomal fraction with 2 ml each of 180 mg/ml glucose-6-phosphate, 25 mg/ml NADP, and 150 mM KCl. CYP2E1 activity of the S9 and microsomal fractions were determined as the activity of chlorzaxazone 6-hydroxylation according to the method of Ikeda et al. [2001].

We grew the cell lines in RPMI1640 medium (Gibco-BRL, Life Technology, Grand Island, NY) supplemented with 10% heat-inactivated horse serum (JRH Biosciences, Lenexa, KS), 200 μg/ml sodium pyruvate, 100 U/ml penicillin, and 100 μg/ml streptomycin, and we maintained the cultures at 10^5-10^6 cells/ml at 37°C in a 5% CO_2 atmosphere with 100% humidity.

umu Assay

The *umu* assay was carried out by the method of Aryal et al. [1999, 2000] with slight modification. Overnight cultures of tester strains were diluted 100-fold with TGlyT medium (1% Bactotryptone, 0.5% NaCl (w/v), 0.2% glycerol (v/v), and 1 μg of tetracycline/ml, 1.0 mM IPTG, 0.5 mM8-ALA, and 250 ml of trace element mixture/l) [Sandhu et al., 1994]. The culture was incubated for 1 hr at 37°C and then 0.75 ml aliquots of TGA culture (OD_{600}: 0.25–0.3) and human. Induction of the *umu*C gene by HCAs in different strains was determined by measuring cellular β-galactosidase activity, as described by Oda et al. [1985]. Cell toxicity was determined in reaction mixture by measuring the optical density change at 600 nm.

Mammalian Cell Assays Measuring Gene Mutation and Chromosome Damage

We incubated 20-ml aliquots of TK6, AHH-1, or h2E1v2 cell suspensions (5.0×10^5 cells/ml) treated with serially diluted AA, GA, or DMN in the presence or absence of S9 or micorosomes at 37°C for 4 hr, washed them once, resuspended them in fresh medium, and cultured them in new flasks for the MN and TK assays. For TK6 cells, we also seeded cells into the 96-well plates (1.6 cells/well) to determine plating efficiency (PE0).

Forty-eight hours after treating the cells, we prepared the MN test samples as previously reported [Koyama et al., 2006]. At least, 1,000 intact interphase cells for each treatment were examined, and the cells containing MN were scored. The MN frequencies between nontreated and treated cells were statistically analyzed by Fisher's exact test. The concentration–response relationship was evaluated by the Cochran-Armitage trend test [Matsushima et al., 1999].

We maintained the cultures another 24 hr to allow phenotypic expression prior to plating for determination of the mutant fractions. After the expression time, to isolate the TK deficient mutants, we seeded the cells into 96-well plates in the presence of 3.0 μg/ml trifluorothymidine (TFT).

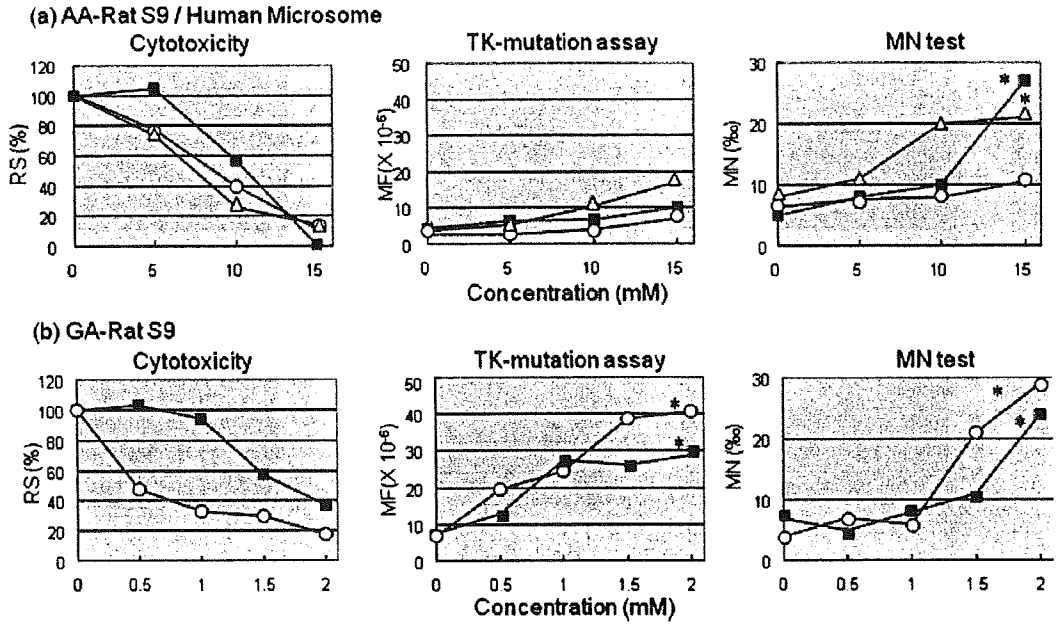

Fig. 1. Cytotoxic (relative survival, RS) and genotoxic (TK and MN assays) responses of TK6 cells treated with AA or GA for 4 hr with or without metabolic activation. (a) TK6 cells were treated with AA without (■) or with (○) rat liver S9 or human microsomes (△). (b) TK6 cells were treated with GA without (■) or with (○) rat liver S9. *$P < 0.05$ (Omori method for TK-mutation assay, trend test for MN assay).

We also seeded cells into the 96-well plates in the absence of TFT to determine plating efficiency (PE3). TK6 cells were seeded at 40,000 cells/well and 1.6 cell/well for TFT and PE plates, respectively. AHH-1 and h2E1v2 cells were seeded at 5,000 cells/well and 3.2 cells/well for TFT and PE plates, respectively. All plates were incubated at 37°C in 5% CO_2 in a humidified incubator. We scored for the colonies in the PE plates at 14th day after plating, and scored for the colonies in the TFT plate on the 28th day after plating. Mutation frequencies were calculated according to the Poisson distribution [Furth et al., 1981]. The data were statistically analyzed by Omori's method, which consists of a modified Dunnett's procedure for identifying clear negative, a Simpson-Margolin procedure for detecting downturn data, and a trend test to evaluate the dose-dependency [Omori et al., 2002]. We evaluated cytotoxicity for TK6 by relative survival (RS), which is calculated from plating efficiency (PE0), and for AHH-1 and h2E1v2 by relative suspension growth (RSG), which is calculated from cell growth rate during 3 days expression period.

Western Blot Analysis

A goat polyclonal anti-rat CYP2E1 antibody (Daiichi Pure Chemical, Tokyo) and rabbit anti-rat actin (Sigma, St. Louis, MO) were used as primary antibodies. AP-conjugated secondary antibody (Cappel, Organon Technika Corp., West Chester, PA) was used to detect primary antibody signals.

DNA Adduct Assay

As a standard for LC/MS/MS analysis, N7-GA-Gua and [$^{15}N_5$]-labeled N7-GA-Gua were synthesized as described previously [Gamboa da Costa et al., 2003]. DNA was extracted from the cells by using DNeasy 96 Blood &Tissue Kit (QIAGEN, Düsseldorf) and incubated at 37°C for 48 hr for deprination. An aliquot of the [$^{15}N_5$]-labeled N7-GA-Gua standard was added to each sample and filtered through an ultrafiltration membrane to remove DNA. The eluted-solution was evaporated thoroughly and dissolved in water, and then the solutions were subsequently quantified by LC/MS/MS.

RESULTS

Cytotoxicity and Genotoxicity of AA and GA Under Metabolic Activation

We used human microsomal preparation and phenobarbital- and 5,6-benzoflavone-treated rat liver S9 for metabolic activation. CYP2E1 activity of the human microsomal preparation was more than twice that of the rat liver S9 preparations (2,917 vs. 1,295 pmol/mg/min).

Figure 1 shows the cytotoxicity (RS; relative survival), MN, and *TK*-mutations induced by AA (a) and GA (b) with and without rat liver S9 or human microsomes. Rat liver S9 or human microsomes enhanced cytotoxicity (RS) of AA and GA. On the other hand, AA showed weak genotoxicity only at relatively high concentrations (>10 mM) without S9, but neither activating system enhanced the weak genotoxicty. GA induced TK-mutations dose-dependently from the low concentration (0.5 mM) and induced MN from 1.5 mM both with and without S9. Thus, neither the rat nor human metabolizing system activated AA or inhibited the expression of GA genotoxicity.

umu Assay Using Strains Expressing Human CYP2E1

We used *S. typhimurium* OY1002/2E1 strain to assess the cell toxicity and genotoxicity of AA at exposures up to 10mM (Fig. 2c). We also examined AA and GA with

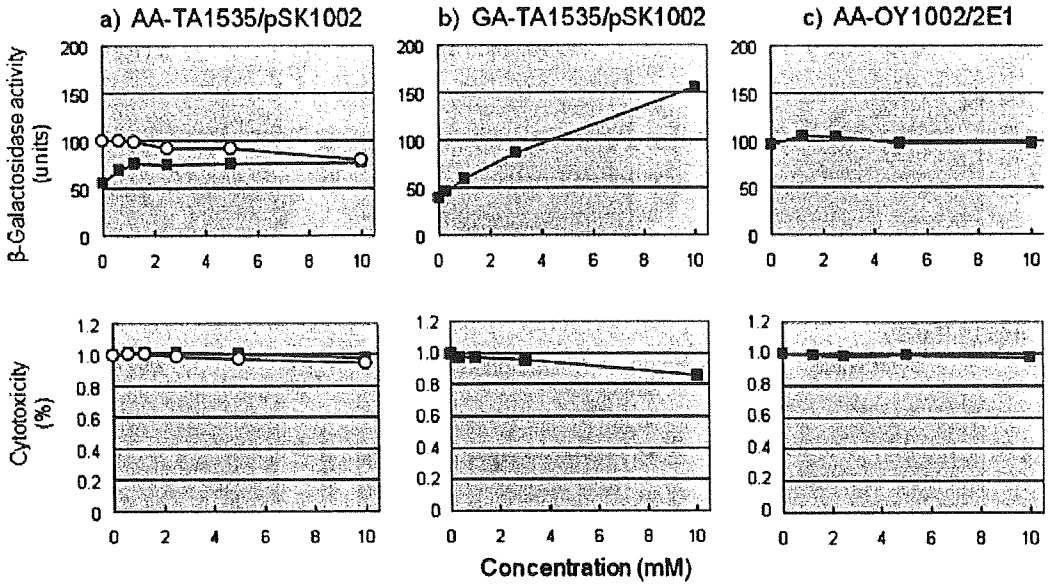

Fig. 2. Induction of *umuC* gene expression and cytotoxic response by AA (a, c) or GA (b) in *S. typhimurium* tester strains TA1535/pSK1002 (a, b) and OY1002/2E1 (c). The *umu* tests were conducted without (■) or with rat S9 (○). β-Galactosidase activity (units) was determined as described in Materials and Methods. Cytotoxic activities are expressed as % optical density change at 600 nm.

or without rat S9 using TA1535/pSK1002 strain. Although GA clearly produced a dose-related increase in response to DNA damage (Fig. 2b), AA elicited no genotoxic or cell toxic response with and without S9 (Fig. 2a). Thus, we could not demonstrate any in vitro genotoxicity of AA in the bacterial system.

Cytotoxic and Genotoxic Responses to AA in Transgenic Cell Lines

Western blot analysis revealed that h2E1v2 accumulated more CYP2E1 than either of its parental cell lines (Fig. 3). Both the h2E1v2 and AHH-1 cells exhibited weak responses (TK-gene mutations and MN) to AA at $\leq$3 mM with little difference in cytotoxicity (RSG, relative suspension growth) (Fig. 4a). h2E1v2 differed from AHH-1, however, in that it showed clear genotoxic and cytotoxic responses (RSG) to DMN, which is a representative substrate for CYP2E1 (Fig. 4b). Thus, the h2E1v2 cell line had CYP2E1 activity but did not activate AA.

DNA Adduct Formation by AA and GA in the Cell Lines

AA induced trace amounts of N7-GA-Gua adduct in TK6 cells (with and without S9) (Fig. 5a) and in AHH-1 and h2E1v2 cells (Fig. 5b). GA, on the other hand, induced a substantial number of N7-GA-Gua adducts in TK6 cells (Fig. 5c). These results suggest that the expression of genotoxicity may be dependent on N7-GA-Gua adduct formation, and the in vitro metabolic activation system did not metabolize AA into GA.

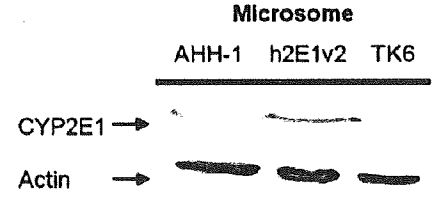

Fig. 3. Western blot analysis of CYP2E1 in AHH-1, h2E1v2, and TK6 cells. Equal amount of materials were loaded for each sample. CYP2E1 protein was stained with the anti-CYP2E1 antibody. Actin was used as a loading control.

DISCUSSION

A large number of studies about the in vitro genotoxicity of AA have been reported [Dearfield et al., 1995; Besaratinia and Pfeifer, 2005]. AA was negative in Ames assay in both the presence and absence of S9 [Zeiger et al., 1987; Knaap et al., 1988; Tsuda et al., 1993]. In mammalian cell assays, cytogenetic tests such as chromosome aberration test and sister chromatid exchange tests were positive [Sofuni et al., 1985; Tsuda et al., 1993]. AA also induced *Tk* mutation in the MLA but did not induce *Hprt* mutation in V79 cells [Moore et al., 1987;

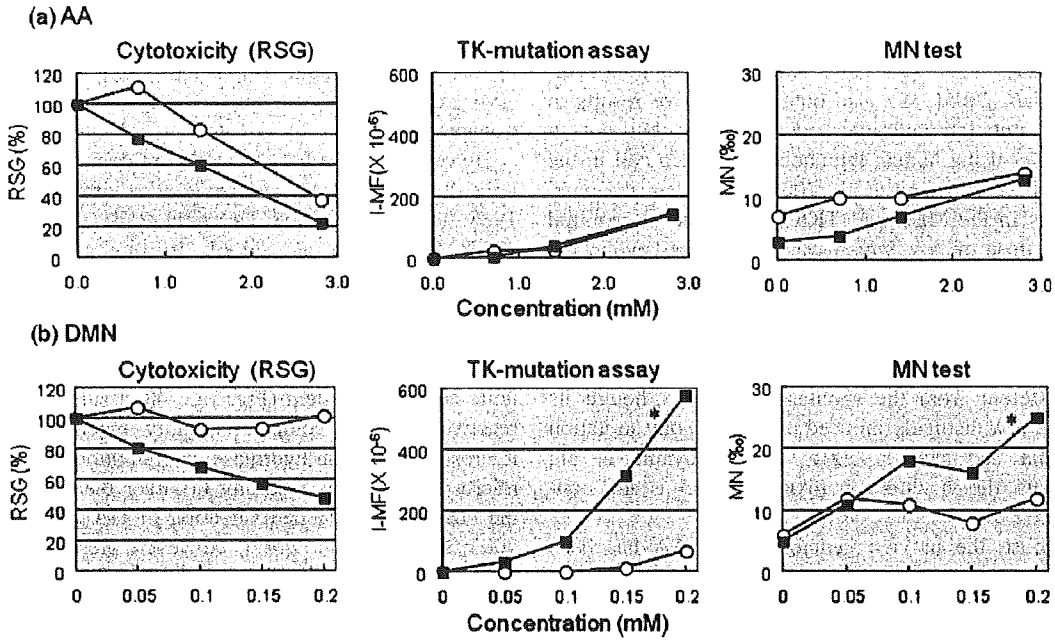

Fig. 4. Cytotoxic (relative suspension growth, RSG) and genotoxic (TK assay and MN test) responses of AHH-1 (○) or h2E1v2 (■) cells treated with AA or DMN for 4 hr. I-MF means induced mutation fraction, in which back ground mutation frequency is subtracted. *$P < 0.05$ (Omori method for TK-mutation assay, trend test for MN assay).

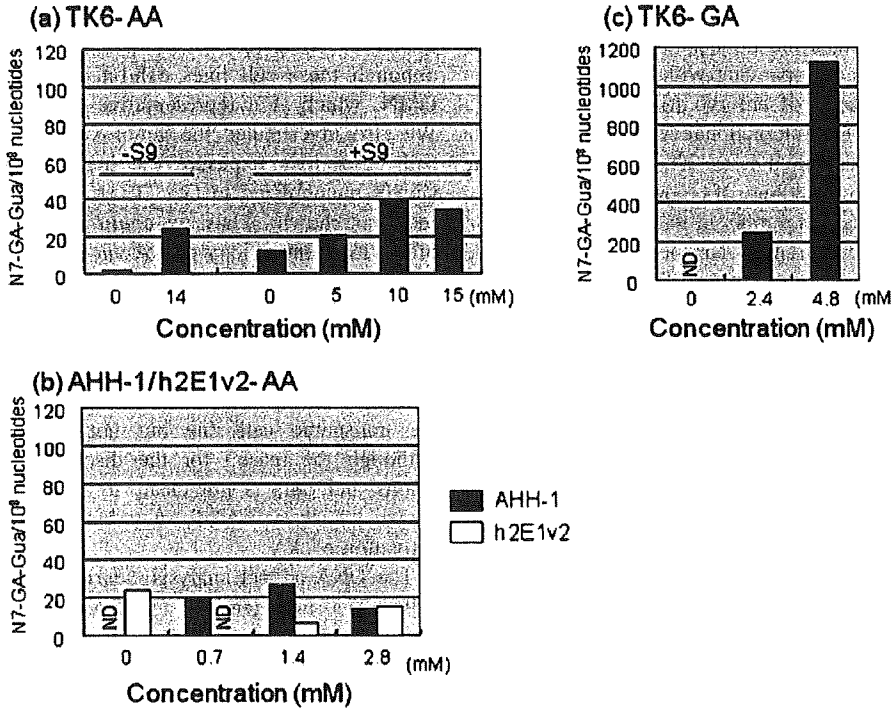

Fig. 5. Levels of N7-GA-Gua adduct in TK6 (a, c), AHH-1 (b), or h2E1v2 (b) cells treated with AA (a, b) or GA (c) for 4 hr at different concentrations. Data are expressed as the number of adducts in 10^8 nucleotides.

Knaap et al., 1988; Tsuda et al., 1993; Baum et al., 2005; Mei et al., 2008], and produced negative results in the Comet assay with V79 cells and human lymphocytes [Baum et al., 2005]. We also obtained positive results in *TK* gene mutation and micronuclei assays, but not in Comet assay using human lymphoblastoid TK6 cell in the absence of S9 [Koyama et al., 2006]. To obtain the positive results in the MLA and TK6 cells, however required very high dose of AA, which was sometimes beyond the top dose of the OECD testing guideline (>10 mM) [Koyama et al., 2006; Mei et al., 2008]. The spectrum of AA-induced *TK* mutations in TK6 and *cII* mutations in Big Blue® mouse embryonic fibroblasts were not significantly different from the spontaneous one, although its metabolite GA distinctly induced a specific point mutation [Besaratinia and Pfeifer, 2003, 2004; Koyama et al., 2006]. Thus, the in vitro genotoxicity of AA is still controversial.

In contrast, the in vivo genotoxicity of AA has been clearly demonstrated by various rodent genotoxicity tests including micronuclei tests in peripheral blood [Cao et al., 1993; Abramsson-Zetterberg, 2003; Manjanatha et al., 2005], transgenic gene mutation in liver [Manjanatha et al., 2005], and Comet assay in various organs [Ghanayem et al., 2005b]. AA has also proven to be genotoxic to germ cells [Dearfield et al., 1995]. AA induced micronuclei in mice spermatids, and heritable chromosome translocations and specific locus mutations in postomeiotic sperm and spermatogonia [Lahdetie et al., 1994; Xiao and Tates, 1994]. AA also elevated the frequency of dominant lethal mutations probably accompanying with chromosome aberrations leading to death of embryo [Shelby et al., 1987; Adler et al., 1994]. The International Agency for Research on Cancer (IARC) classified it as 2A, a probable human carcinogen based on finding of rodent carcinogenicity [IARC, 1994]. AA caused tumors in various organs including mammary gland, peritesticular mesothelium, thyroid, and central nervous system [Carere, 2006], although the AA-inducing genotoxicity in these organs have not been demonstrated.

AA is metabolized either via direct glutathione conjugation followed by excretion of mercapturic acid or via oxidative pathways catalyzed by CYP2E1 to yield GA [Calleman et al., 1990; Wu et al., 1993; Sumner et al., 1999]. GA reacts quickly with DNA, mainly forming N7-GA-Gua adduct. Genotoxicity of GA has been demonstrated in vitro and in vivo. In contrast to AA, GA is positive in most genotoxicity tests [Hashimoto and Tanii, 1985; Dearfield et al., 1995; Besaratinia and Pfeifer, 2004; Baum et al., 2005; Koyama et al., 2006]. Manjanatha et al. [2005] demonstrated in transgenic Big Blue® mice that both AA and GA induces endogenous *Hprt* and transgenic *cII* mutation at same level, and also produced similar mutational spectra. The predominant type of mutations observed in these two systems was G:C to T:A transversion, which is presumably derived from N7-GA-Gua [Besaratinia and Pfeifer, 2005]. The in vivo results with transgenic Big Blue® mice indicate that in vivo expression of AA genotoxicity is mediated via its GA metabolite.

However, no one has succeeded in demonstrating metabolically activated AA genotoxicity in vitro [Knaap et al., 1988; Tsuda et al., 1993; Dearfield et al., 1995; Friedman, 2003; Emmert et al., 2006]. In this study, we used induced rat liver S9 and human microsomal fraction for the metabolic activation. Although they have high CYP2E1 activity, the AA-inducing genotoxicity was never influenced by the presence of the exogenous metabolic activation system (Fig. 1a). We assumed that GA, a reactive epoxide, could be rapidly inactivated through microsomal epoxide hydrolase or glutathione in any S9 or microsomal fraction resulting in either the metabolism or the conjugation and detoxification of GA [Sumner et al., 2003; Decker et al., 2009]. However, presence of rat S9 did not prevent GA from inducing *TK*-mutation and micronuclei.

The *umu* assay could not detect the genotoxicity of AA even by the strain (Fig. 2). Emmert et al. [2006] also failed to demonstrate the mutagenicity of AA in the Ames test using the metabolically competent *S. typhimurium strain* YG7108pinERb$_5$ that expresses CYP2E1. In mammalian cell system, such as the human lymphoblastoid cell line, h2E1v2 overexpressing human CYP2E1 did not show different response in *TK*-gene mutation and MN induction compared to its parental cell line, AHH-1, although these cell lines exhibited distinct difference to DMN, which is a representative substrate for CYP2E1. We also investigated the genotoxicity of AA in h2E1v2 cells after long exposure (24 hr), because AA may be slowly metabolized to GA. The result was also negative (data not shown). Thus, we could not obtain any evidence of in vitro genotoxicity of AA *via* metabolic activation.

Glatt et al. [2005] developed a Chinese hamster V79-derived cell line that stably expresses human CYP2E1 and sulphotransferase (SULT), and applied it to investigate sister chromatid exchanges (SCE) induced by some chemicals. They demonstrated that AA induced SCE in the transgenic cell line but not in the parental line. Although the reason for the discrepancy between their results and ours is not clear, it is possible that another enzyme, such as SULT, may be involved in metabolic activation of AA.

The DNA adduct analysis clearly revealed that h2E1v2 cells does not generate N7-GA-Gua adduct in vitro. Because exposure of human cells to GA results in significant accumulation of N7-GA-Gua adduct, but DNA adduct analysis following exposure of h2E1v2 with AA does not generate N7-GA-Gua adduct in vitro, lead one a conclusion that the presence of CYP2E1 alone is not enough to metabolize AA to GA in mammalian cells. The

DNA adduct analysis also strongly supports a hypothesis that GA contribute to its genotoxicity by forming N7-GA-Gua adduct. Interestingly, very small amount of N7-GA-Gua adduct was generated in TK6 cells in a dose-dependent manner regardless of the presence of S9 (Fig. 5a). TK6 cells themselves may have an enzymatic activity to metabolize AA to GA, although its activity must be extremely low. Ghanayem et al. [2005b] showed that AA was not mutagenic or genotoxic in CYP2E1-null mice. Intraperitoneal injection of AA (25, 50 mg/kg) by once daily for 5 days induced micronuclei in erythrocyte and DNA damage assessed by Comet assay in leukocyte and liver cells of wild-type, but not in the CYP2E1-null mice. The plasma concentration of AA in the CYP2E1-null mice was 115-times higher than in the wild-type mice, while the GA concentration in the CYP2E1-null mice was negligible compared to that in the wild-type mice [Ghanayem et al., 2000]. Ghanayem et al. [2005c] also demonstrated that AA produces dominant lethal in mice that express CYP2E1, but not in mice that do not express CYP2E1, indicating that induction of germ cell mutations by AA in mice in vivo is also dependent upon CYP2E1 metabolism. These results clearly suggest that CYP2E1 is the principal enzyme responsible for the metabolism of AA to GA in vivo.

In conclusion, AA could not be metabolized to GA by in vitro metabolic activation system commonly used in genotoxicity tests. In vivo, on the other hand, GA is apparently responsible for AA-inducing genotoxicity. Although AA may exhibit genotoxicity in in vitro mammalian cells at high concentrations, its positive response is not relevant for its major genotoxicity. AA could be classified into in vivo specific genotoxic chemical.

ACKNOWLEDGMENT

We thank Dr. Crespi (BD Bio Sciences) for kindly providing the AHH-1 and h2E1v2 cell lines.

REFERENCES

Abramsson-Zetterberg L. 2003. The dose-response relationship at very low doses of acrylamide is linear in the flow cytometer-based mouse micronucleus assay. Mutat Res 535:215–222.

Adler ID, Reitmeir P, Schmoller R, Schriever-Schwemmer G. 1994. Dose response for heritable translocations induced by acrylamide in spermatids of mice. Mutat Res 309:285–291.

Aryal P, Yoshikawa K, Terashita T, Guengerich FP, Shimada T, Oda Y. 1999. Development of a new genotoxicity test system with *Salmonella typhimurium* OY1001/1A2 expressing human CYP1A2 and NADPH-P450 reductase. Mutat Res 442:113–120.

Aryal P, Terashita T, Guengerich FP, Shimada T, Oda Y. 2000. Use of genetically engineered *Salmonella typhimurium* OY1002/1A2 strain coexpressing human cytochrome P450 1A2 and NADPH-cytochrome P450 reductase and bacterial *O*-acetyltransferase in SOS/umu assay. Environ Mol Mutagen 36:121–126.

Baum M, Fauth E, Fritzen S, Herrmann A, Mertes P, Merz K, Rudolphi M, Zankl H, Eisenbrand G. 2005. Acrylamide and glycidamide: Genotoxic effects in V79-cells and human blood. Mutat Res 580:61–69.

Besaratinia A, Pfeifer GP. 2003. Weak yet distinct mutagenicity of acrylamide in mammalian cells. J Natl Cancer Inst 95:889–896.

Besaratinia A, Pfeifer GP. 2004. Genotoxicity of acrylamide and glycidamide. J Natl Cancer Inst 96:1023–1029.

Besaratinia A, Pfeifer GP. 2005. DNA adduction and mutagenic properties of acrylamide. Mutat Res 580:31–40.

Calleman CJ, Bergmark E, Costa LG. 1990. Acrylamide is metabolized to glycidamide in the rat: Evidence from hemoglobin adduct formation. Chem Res Toxicol 3:406–412.

Cao J, Beisker W, Nusse M, Adler ID. 1993. Flow cytometric detection of micronuclei induced by chemicals in poly- and normochromatic erythrocytes of mouse peripheral blood. Mutagen 8:533–541.

Carere A. 2006. Genotoxicity and carcinogenicity of acrylamide: A critical review. Ann Ist Super Sanita 42:144–155.

Crespi CL, Thilly WG. 1984. Assay for gene mutation in a human lymphoblast line, AHH-1, competent for xenobiotic metabolism. Mutat Res 128:221–230.

Crespi CL, Langenbach R, Penman BW. 1993a. Human cell lines, derived from AHH-1 TK+/- human lymphoblasts, genetically engineered for expression of cytochromes P450. Toxicology 82:89–104.

Crespi CL, Penman BW, Gonzalez FJ, Gelboin HV, Galvin M, Langenbach R. 1993b. Genetic toxicology using human cell lines expressing human P-450. Biochem Soc Trans 21:1023–1028.

Dearfield KL, Douglas GR, Ehling UH, Moore MM, Sega GA, Brusick DJ. 1995. Acrylamide: A review of its genotoxicity and an assessment of heritable genetic risk. Mutat Res 330:71–99.

Decker M, Arand M, Cronin A. 2009. Mammalian epoxide hydrolases in xenobiotic metabolism and signalling. Arch Toxicol 83:297–318.

Doerge DR, da Costa GG, McDaniel LP, Churchwell MI, Twaddle NC, Beland FA. 2005. DNA adducts derived from administration of acrylamide and glycidamide to mice and rats. Mutat Res 580:131–141.

Emmert B, Bunger J, Keuch K, Muller M, Emmert S, Hallier E, Westphal GA. 2006. Mutagenicity of cytochrome P450 2E1 substrates in the Ames test with the metabolic competent *S. typhimurium* strain YG7108pin3ERb5. Toxicology 228:66–76.

Friedman M. 2003. Chemistry, biochemistry, and safety of acrylamide. A review. J Agric Food Chem 51:4504–4526.

Furth EE, Thilly WG, Penman BW, Liber HL, Rand WM. 1981. Quantitative assay for mutation in diploid human lymphoblasts using microtiter plates. Anal Biochem 110:1–8.

Gamboa da Costa G, Churchwell MI, Hamilton LP, Von Tungeln LS, Beland FA, Marques MM, Doerge DR. 2003. DNA adduct formation from acrylamide via conversion to glycidamide in adult and neonatal mice. Chem Res Toxicol 16:1328–1337.

Ghanayem BI, Hoffler U. 2007. Investigation of xenobiotics metabolism, genotoxicity, and carcinogenicity using Cyp2e1(-/-) mice. Curr Drug Metab 8:728–749.

Ghanayem BI, Wang H, Sumner S. 2000. Using cytochrome P-450 gene knock-out mice to study chemical metabolism, toxicity, and carcinogenicity. Toxicol Pathol 28:839–850.

Ghanayem BI, McDaniel LP, Churchwell MI, Twaddle NC, Snyder R, Fennell TR, Doerge DR. 2005a. Role of CYP2E1 in the epoxidation of acrylamide to glycidamide and formation of DNA, hemoglobin adducts. Toxicol Sci 88:311–318.

Ghanayem BI, Witt KL, Kissling GE, Tice RR, Recio L. 2005b. Absence of acrylamide-induced genotoxicity in CYP2E1-null mice: Evidence consistent with a glycidamide-mediated effect. Mutat Res 578:284–297.

Ghanayem BI, Witt KL, El-Hadri L, Hoffler U, Kissling GE, Shelby MD, Bishop JB. 2005c. Comparison of germ cell mutagenicity in male CYP2E1-null and wild-type micetreated with acrylamide: Evidence supporting a glycidamide-mediated effect. Biol Reprod 72:157–163.